

# 7 Chemistry and Properties of Phenolic Resins and Networks

*S. Lin-Gibson*

Polymers Division, NIST, Gaithersburg, Maryland 20899-8543

*J. S. Riffle*

Department of Chemistry, Virginia Polytechnic Institute and State University, Blacksburg, Virginia 24061

## 7.1 INTRODUCTION

Phenolic resins comprise a large family of oligomers and polymers (Table 7.1), which are various products of phenols reacted with formaldehyde. They are versatile synthetic materials with a large range of commercial applications. Plywood adhesives account for nearly half of all phenolic applications while wood-binding and insulation materials also make up a significant portion.<sup>1</sup> Other uses for phenolics include coatings, adhesives, binders for abrasives, automotive and electrical components, electronic packaging, and matrices for composites.

Phenolic oligomers are prepared by reacting phenol or substituted phenols with formaldehyde or other aldehydes. Depending on the reaction conditions (e.g., pH) and the ratio of phenol to formaldehyde, two types of phenolic resins are obtained. Novolacs are derived from an excess of phenol under neutral to acidic conditions, while reactions under basic conditions using an excess of formaldehyde result in resoles.

Phenolic resins were discovered by Baeyer in 1872 through acid-catalyzed reactions of phenols and acetaldehyde. Kleeberg found in 1891 that resinous products could also be formed by reacting phenol with formaldehyde. But it was Baekeland who was granted patents in 1909 describing both base-catalyzed resoles (known as Bakelite resins) and acid-catalyzed novolac products.<sup>2</sup>

This chapter emphasizes the recent mechanistic and kinetic findings on phenolic oligomer syntheses and network formation. The synthesis and characterization of both novolac- and resole-type phenolic resins and their resulting networks are described. Three types of networks, novolac-hexamethylenetetramine (HMTA),

**TABLE 7.1 U.S. Phenolic Production (in millions of pounds on a gross weight basis)<sup>a</sup>**

1998	1997	% Change
3940	3734	5.5

<sup>a</sup>From Society of Plastic Industries Facts and Figures, SPI, Washington, DC, 1999.

novolac-epoxies, and thermally cured resoles will be primarily discussed. Other phenolic-based networks include benzoxazines and cyanate esters. Since phenolic materials possess excellent flame retardance, a discussion of the thermal and thermo-oxidative degradation pathways will be included. Detailed information on the chemistry, applications, and processing of phenolic materials can be found in a number of references.<sup>2-6</sup>

## 7.2 MATERIALS FOR THE SYNTHESIS OF NOVOLAC AND RESOLE PHENOLIC OLIGOMERS

### 7.2.1 Phenols

The most common precursor to phenolic resins is phenol. More than 95% of phenol is produced via the cumene process developed by Hock and Lang (Fig. 7.1). Cumene is obtained from the reaction of propylene and benzene through acid-catalyzed alkylation. Oxidation of cumene in air gives rise to cumene hydroperoxide, which decomposes rapidly at elevated temperatures under acidic conditions to form phenol and acetone. A small amount of phenol is also derived from coal.

Substituted phenols such as cresols, *p*-*tert*-butylphenol, *p*-phenylphenol, resorcinol, and cardanol (derived from cashew nut shells) have also been used as precursors for phenolic resins. Alkylphenols with at least three carbons in the substituent lead to more hydrophobic phenolic resins that are compatible with many oils, natural resins, and rubbers.<sup>7</sup> Such alkylphenolic resins are used as modifying and crosslinking agents for oil varnishes, as coatings and printing inks, and as antioxidants and stabilizers. Bisphenol-A (2,2-*p*-hydroxyphenylpropane),

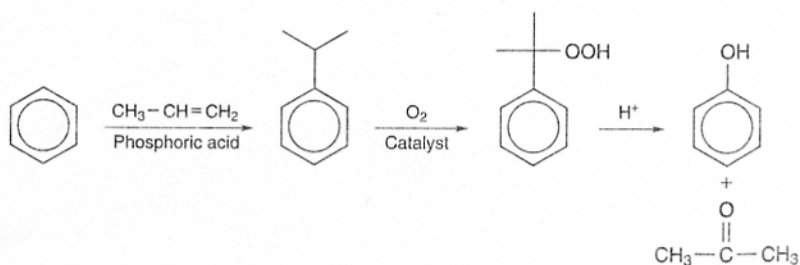


Figure 7.1 Preparation of phenol monomer.

a precursor to a number of phenolic resins, is the reaction product of phenol and acetone under acidic conditions.

An additional activating hydroxyl group on the phenolic ring allows resorcinol to react rapidly with formaldehyde even in the absence of catalysts.<sup>8</sup> This provides a method for room temperature cure of resorcinol-formaldehyde resins or mixed phenol-formaldehyde/resorcinol-formaldehyde resins. Trihydric phenols have not achieved commercial importance, probably due to their higher costs.

### 7.2.2 Formaldehyde and Formaldehyde Sources

Formaldehyde, produced by dehydrogenation of methanol, is used almost exclusively in the synthesis of phenolic resins (Fig. 7.2). Iron oxide, molybdenum oxide, or silver catalysts are typically used for preparing formaldehyde. Air is a safe source of oxygen for this oxidation process.

Since formaldehyde is a colorless pungent irritating gas, it is generally marketed as a mixture of oligomers of polymethylene glycols either in aqueous solutions (formalin) or in more concentrated solid forms (paraformaldehyde). The concentration of formalin ranges between about 37 and 50 wt %. A 40 wt % aqueous formalin solution at 35°C typically consists of methylene glycols with 1–10 repeat units. The molar concentration of methylene glycol with one repeat unit (HO-CH<sub>2</sub>-OH) is highest and the concentrations decrease with increasing numbers of repeat units.<sup>9</sup> Paraformaldehyde, a white solid, contains mostly polymethylene glycols with 10–100 repeat units. It is prepared by distilling aqueous formaldehyde solutions and generally contains 1–7 wt % water.

Methanol, the starting reagent for producing formaldehyde, stabilizes the formalin solution by forming acetal endgroups and is usually present in at least small amounts (Fig. 7.3). Methanol may also be formed by disproportionation during storage. The presence of methanol reduces the rate of phenol-formaldehyde reaction but does not affect the activation energies.<sup>10</sup> It is generally removed by stripping at the end of the reaction.

Water is necessary for decomposing paraformaldehyde to formaldehyde (Fig. 7.4). However, water can serve as an ion sink and water-phenol mixtures

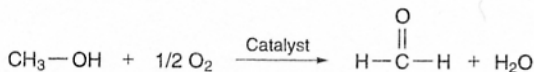


Figure 7.2 Synthesis of formaldehyde.



Figure 7.3 Formation of hemiformals.



Figure 7.4 Depolymerization of aqueous polyoxymethylene glycol.



Figure 7.5 Synthesis of HMTA.

phase separate as the water concentration increases. Therefore, large amounts of water reduce the rate of reaction between phenol and formaldehyde.<sup>11</sup>

Used for crosslinking novolacs or catalyzing resole syntheses, HMTA is prepared by reacting formaldehyde with ammonia (Fig. 7.5). The reaction is reversible at high temperatures, especially above 250°C. HMTA can also be hydrolyzed in the presence of water.

### 7.3 NOVOLAC RESINS

The most common precursors for preparing novolac oligomers and resins are phenol, formaldehyde sources, and, to a lesser extent, cresols. Three reactive sites for electrophilic aromatic substitution are available on phenol which give rise to three types of linkages between aromatic rings, that is, ortho-ortho, ortho-para, and para-para. The complexity of the isomers leads to amorphous materials. For a novolac chain with 10 phenol groups, 13,203 isomers<sup>12</sup> can statistically form, making the separation of pure phenolic compounds from novolacs nearly impossible.

#### 7.3.1 Synthesis of Novolac Resins

Novolacs are prepared with an excess of phenol over formaldehyde under acidic conditions (Fig. 7.6). A methylene glycol is protonated by an acid from the reaction medium, which then releases water to form a hydroxymethylene cation (step 1 in Fig. 7.6). This ion hydroxyalkylates a phenol via electrophilic aromatic substitution. The rate-determining step of the sequence occurs in step 2 where a pair of electrons from the phenol ring attacks the electrophile forming a carbocation intermediate. The methylol group of the hydroxymethylated phenol is unstable in the presence of acid and loses water readily to form a benzylic carbonium ion (step 3). This ion then reacts with another phenol to form a methylene bridge in another electrophilic aromatic substitution. This major process repeats until the formaldehyde is exhausted.

The reaction between phenol and formaldehyde is exothermic. Therefore, the temperature must be controlled to prevent the buildup of heat, particularly during the early stages of reaction.<sup>4</sup> When formalin is used, water provides a medium for heat dissipation.

Typical formaldehyde-to-phenol ratios in novolac syntheses range from about 0.7 to 0.85 to maintain oligomers with sufficiently low molecular weights

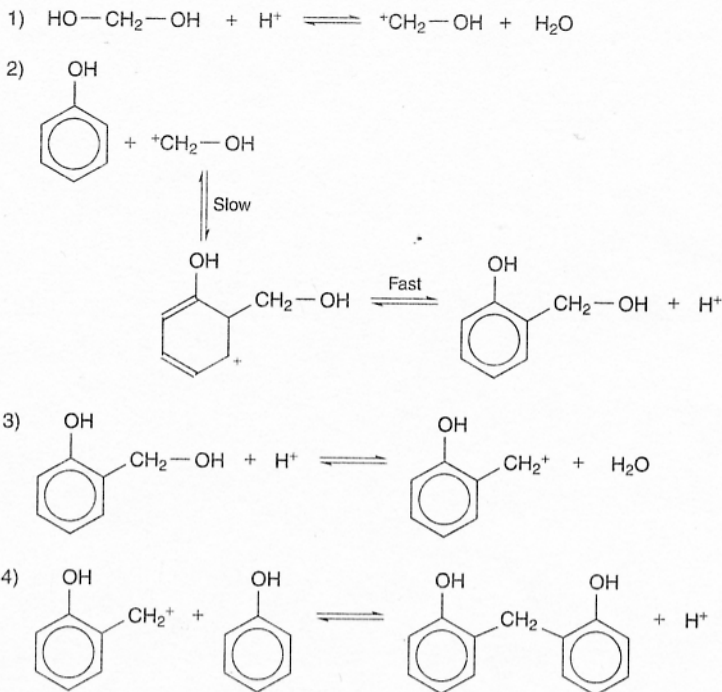


Figure 7.6 Mechanism of novolac synthesis via electrophilic aromatic substitution.

and reasonable melt viscosities. This is especially important since phenol is trifunctional and a gel fraction begins to form as conversion increases. As a result, the number-average molecular weights ( $M_n$ ) of novolac resins are generally below 1000 g/mol.

The acidic catalysts used for these reactions include formic acid, HX (X = F, Cl, Br), oxalic acid, phosphoric acid, sulfuric acid, sulfamic acid, and *p*-toluenesulfonic acid.<sup>4</sup> Oxalic acid is preferred since resins with low color can be obtained. Oxalic acid also decomposes at high temperatures (>180°C) to CO<sub>2</sub>, CO, and water, which facilitates the removal of this catalyst thermally. Typically, 1–6 wt % catalyst is used. Hydrochloric acid results in corrosive materials and reportedly releases carcinogenic chloromethyl ether by-products during resin synthesis.<sup>2</sup>

Approximately 4–6 wt % phenol can typically be recovered following novolac reactions. Free phenol can be removed by washing with water repeatedly. The recovered phenolic components may contain 1,3-benzodioxane, probably derived from benzyl hemiformals (Fig. 7.7).<sup>2</sup>

### 7.3.2 "High-Ortho" Novolac Resins

High-ortho novolacs (Fig. 7.8) are sometimes more desirable since they cure more rapidly with HMTA. A number of oxides, hydroxides, or organic salts of electropositive metals increase the reactivity of the ortho position during

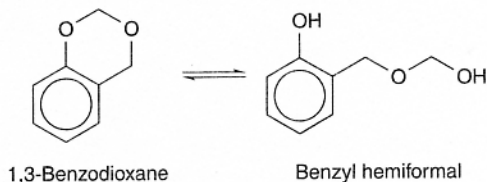


**Figure 7.7** By-products of novolac synthesis.

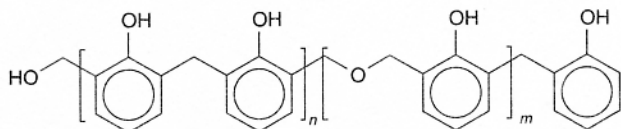


**Figure 7.8** High ortho novolacs.

oligomer formation.<sup>13</sup> These high ortho novolacs are typically formed at pH 4–6 as opposed to the more common strongly acidic conditions.

Metal hydroxides of first- and second-group elements can enhance ortho substitution, the degree of which depends on the strength of metal-chelating effects linking the phenolic oxygen with the formaldehyde as it approaches the ortho position. Transition metal ions of elements such as Fe, Cu, Cr, Ni, Co, Mn, and Zn as well as boric acid also direct ortho substitutions via chelating effects (Fig. 7.9).

Phenol–formaldehyde reactions catalyzed by zinc acetate as opposed to strong acids have been investigated, but this results in lower yields and requires longer reaction times. The reported ortho–ortho content yield was as high as 97%. Several divalent metal species such as Ca, Ba, Sr, Mg, Zn, Co, and Pb combined with an organic acid (such as sulfonic and/or fluoroboric acid) improved the reaction efficiencies.<sup>14</sup> The importance of an acid catalyst was attributed to facilitated decomposition of any dibenzyl ether groups formed in the process. It was also found that reaction rates could be accelerated with continuous azeotropic removal of water.

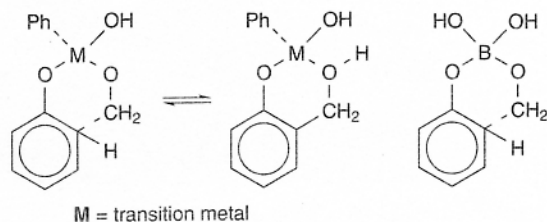


**Figure 7.9** Proposed chelate structures in the synthesis of high ortho novolac oligomers.

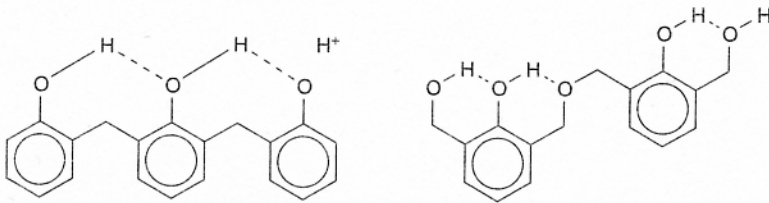


Figure 7.10 Intramolecular hydrogen bonding of high ortho novolacs.

An interesting aspect of high-ortho novolac oligomers is their so-called 'hyperacidity'. The enhanced acidity of high-ortho novolac resins, intermediate between phenols and carboxylic acids, has been attributed to increased dissociation of the phenol protons due to strong intramolecular hydrogen bonding (Fig. 7.10). These materials are also reported to form strong complexes with di- and trivalent metals and nonmetals.<sup>2</sup>

### 7.3.3 Model Phenolic Oligomer Synthesis

Linear novolac oligomers containing only ortho linkages were prepared using bromomagnesium salts under dry conditions.<sup>15</sup> The bromomagnesium salt of phenol coordinates with the incoming formaldehyde (Fig. 7.11a) or quinone methide (Fig. 7.11b) directing the reaction onto only ortho positions.

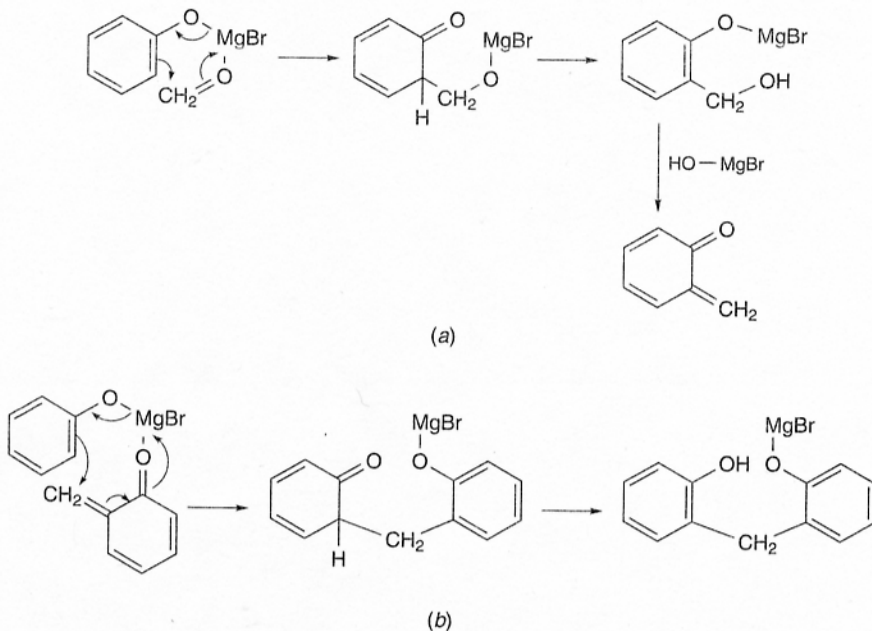


Figure 7.11 Selective ortho coupling reaction using bromomagnesium salts.

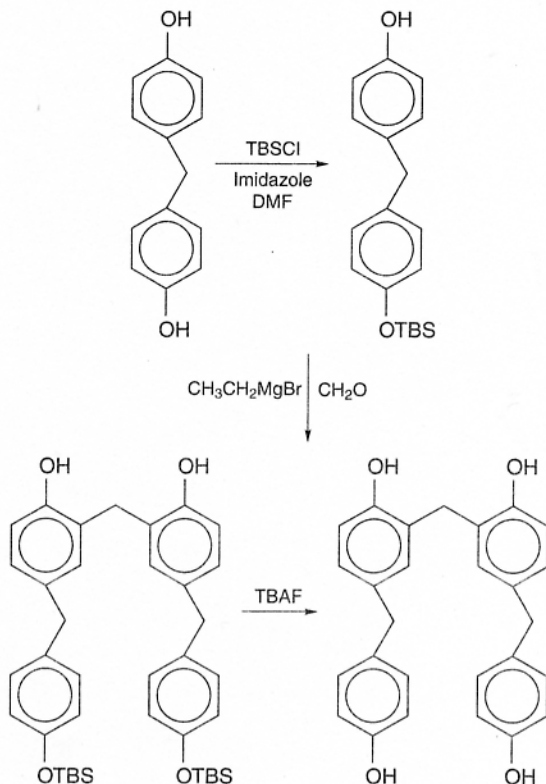
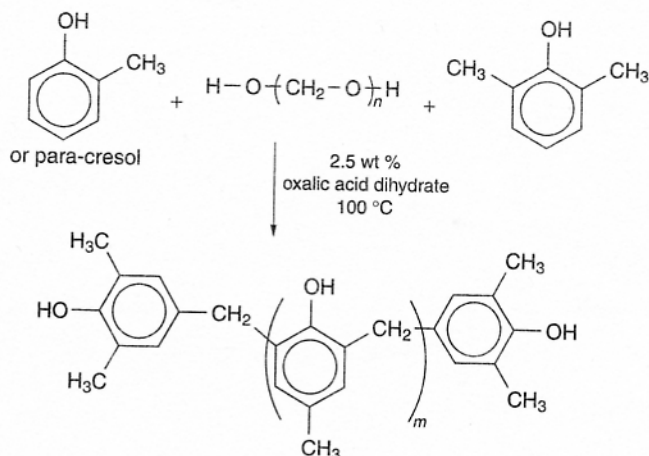


Figure 7.12 Synthesis of model phenolic compound.

de Bruyn et al.<sup>16</sup> prepared low molecular weight model novolac compounds comprised of four to eight phenolic units utilizing the bromomagnesium salt methodology (Fig. 7.12). A para-para-linked dimer was used as the starting material where *tert*-butyldimethylsilyl chloride (TBSCl) was reacted with one phenol on a dimer to deactivate its ring against electrophilic reaction with formaldehyde. Selective ortho coupling formed bridges between the remaining phenol rings; then the *tert*-butyldimethylsilyl protecting groups were removed with fluoride ion. These compounds and all ortho-linked model compounds prepared using bromomagnesium salts were subsequently used as molecular weight standards for calibrating gel permeation chromatography and to study model reactions with HMTA (see Section 7.3.8).

#### 7.3.4 Controlled Molecular Weight Cresol Novolac Oligomers

Although molecular weights in typical phenolic novolac syntheses are intentionally limited, these procedures lack molecular weight control. The reactions are generally terminated prior to full conversion after a certain reaction time or



**Figure 7.13** Synthesis of 2,6-dimethylphenol end-capped cresol novolac resin.

once a specified viscosity is reached. The synthesis of linear controlled molecular weight cresol novolac resins has been investigated by strategically controlling the stoichiometric ratio of cresol to 2,6-dimethylphenol (as the end-capping reagent) as calculated via the Carothers equation (Fig. 7.13) and reacting the materials until full conversion is achieved.<sup>17</sup> Targeted molecular weights could be obtained by using a slight excess of formaldehyde relative to the calculated values. The reasons for needing an excess of formaldehyde were attributed to some reagent loss during the early exothermic reaction stages and also to formation of a small amount of dimethylene ether linkages between cresol rings (thus using 2 mol of formaldehyde in one link as opposed to 1 mol).

The molecular weights were analyzed via <sup>13</sup>C nuclear magnetic resonance (NMR) by ratioing the methyl peaks on endgroups versus the methyl peaks within the repeat units. The molecular weights for these novolac resins made with ortho- or para-cresol showed good agreement between experimental results and the targeted values (Table 7.2).

**TABLE 7.2** Calculated  $M_n$  versus Targeted  $M_n$

Target $M_n$ (g/mol)	$N_{AA}$ (cresol) (mol)	$N_{ZA}$ : (2,6-DMP) <sup>a</sup> (mols)	Ortho Series $M_n$ (g/mol)	Para Series $M_n$ (g/mol)
500	1	0.984	490	510
1000	1	0.323	930	1010
1500	1	0.193	1380	1460
2000	1	0.138	2250	2150

<sup>a</sup>2,6-Dimethylphenol.

### 7.3.5 Reaction Conditions and Copolymer Effects

Alkyl-substituted phenols have different reactivities than phenol toward reaction with formaldehyde. Relative reactivities determined by monitoring the disappearance of formaldehyde in phenol-paraformaldehyde reactions (Table 7.3) show that, under basic conditions, meta-cresol reacts with formaldehyde approximately three times faster than phenol while ortho- and para-cresols react at approximately one-third the rate of phenol.<sup>18</sup> Similar trends were observed for the reactivities of acid-catalyzed phenolic monomers with formaldehyde.

One comparison study of oxalic-acid-catalyzed reactions involving ortho- and meta-cresol mixtures demonstrated that meta-cresol was preferentially incorporated into the oligomers during the early stages of reaction.<sup>19</sup> Given the same reaction conditions and time, higher *o*-cresol compositions (of the mixtures) resulted in decreased overall yields since there was insufficient time for *o*-cresol to fully react. Consequently, the molecular weights and glass transition temperatures ( $T_g$ ) were also lower in these partially reacted materials. As expected, the molecular weight increased if a larger amount of catalyst was used or if more time was allowed for reaction. Increased catalyst concentrations also broadened molecular weight distributions.

Bogan et al. conducted similar studies in which meta- and/or para-cresols were reacted with formaldehyde at 99°C for 3 h using oxalic acid dihydrate as the catalyst to form novolac-type structures.<sup>20</sup> Using a relative reactivity of  $0.09 \pm 0.03$  for *p*-cresol with formaldehyde versus *m*-cresol with formaldehyde, a statistical model was employed to predict the amounts of unreacted cresols during the reactions, branching density, and *m/p*-cresol copolymer compositions. Good agreement was found between the predictions and experimental results. Since *p*-cresol reacted much slower than *m*-cresol, it was to a first approximation considered an unreactive diluent. When meta- and para-cresol mixtures were reacted, oligomers consisting of mostly *m*-cresol formed first; then when the *m*-cresol content was depleted, *p*-cresol incorporation was observed (mostly at the

**TABLE 7.3** Relative Reaction Rates of Various Phenols with Formaldehyde under Basic Conditions<sup>a</sup>

Compound	Relative Reactivity
2,6-Xylenol	0.16
ortho-Cresol	0.26
para-Cresol	0.35
2,5-Xylenol	0.71
3,4-Xylenol	0.83
Phenol	1.00
2,3,5-Trimethylphenol	1.49
meta-Cresol	2.88
3,5-Xylenol	7.75

<sup>a</sup>From ref. 3.

chain ends). Full conversions were not achieved in these investigations, probably due to insufficient reaction times for *p*-cresol to react completely.

Linear novolac resins prepared by reacting para-alkylphenols with paraformaldehyde are of interest for adhesive tackifiers. As expected for step-growth polymerization, the molecular weights and viscosities of such oligomers prepared in one exemplary study increased as the ratio of formaldehyde to para-nonylphenol was increased from 0.32 to 1.00.<sup>21</sup> As is usually the case, however, these reactions were not carried out to full conversion, and the measured  $M_n$  of an oligomer prepared with an equimolar phenol-to-formaldehyde ratio was 1400 g/mol. Plots of apparent shear viscosity versus shear rate of these *p*-nonylphenol novolac resins showed non-Newtonian rheological behavior.

Reaction media play an important role in *m*-cresol-paraformaldehyde reactions.<sup>22</sup> Higher molecular weight resins, especially those formed from near-equimolar *m*-cresol-formaldehyde ratios, can be obtained by introducing a water miscible solvent such as ethanol, methanol, or dioxane to the reaction. Small amounts of solvent (0.5 mol solvent/mol cresol) increased reaction rates by reducing the viscosity and improving homogeneity. Further increases in solvent, however, diluted the reagent concentrations to an extent that decreased the rates of reaction.

### 7.3.6 Molecular Weight and Molecular Weight Distribution Calculations

The molecular weights and molecular weight distributions (MWD) of phenolic oligomers have been evaluated using gel permeation chromatography (GPC),<sup>23,24</sup> NMR spectroscopy,<sup>25</sup> vapor pressure osmometry (VPO),<sup>26</sup> intrinsic viscosity,<sup>27</sup> and more recently matrix-assisted laser desorption/ionization time-of-flight mass spectrometry (MALDI-TOF MS).<sup>28</sup>

The most widely used molecular weight characterization method has been GPC, which separates compounds based on hydrodynamic volume. State-of-the-art GPC instruments are equipped with a concentration detector (e.g., differential refractometer, UV, and/or IR) in combination with viscosity or light scattering. A viscosity detector provides in-line solution viscosity data at each elution volume, which in combination with a concentration measurement can be converted to specific viscosity. Since the polymer concentration at each elution volume is quite dilute, the specific viscosity is considered a reasonable approximation for the dilute solution's intrinsic viscosity. The plot of  $\log[\eta]M$  versus elution volume (where  $[\eta]$  is the intrinsic viscosity) provides a universal calibration curve from which absolute molecular weights of a variety of polymers can be obtained. Unfortunately, many reported analyses for phenolic oligomers and resins are simply based on polystyrene standards and only provide relative molecular weights instead of absolute numbers.

Dargaville et al.<sup>29</sup> and Yoshikawa et al.<sup>23</sup> recognized the difficulties in obtaining accurate GPC molecular weights of phenolic resins due to large amounts of isomers and their associated differences in hydrodynamic sizes. These workers generated GPC calibration curves using a series of low-molecular-weight

model novolac compounds: (1) linear compounds with only ortho-ortho methylene linkages, (2) compounds with ortho-ortho methylene-linked backbones and where each unit had a pendent para-para methylene-linked unit, and (3) compounds with ortho-ortho methylene-linked backbones and where each unit had a pendent para-ortho methylene-linked unit.<sup>29</sup> For a given molecular weight, the hydrodynamic volume of oligomers with only the ortho-ortho methylene links was smaller than the others. It was reasoned that the reduced hydrodynamic volume was caused by "extra" intramolecular hydrogen bonding in high-ortho novolacs, which was a similar argument to that suggested previously by Yoshikawa et al.<sup>23</sup> Based on the GPC calibration curves of the model compounds and their known chemical structures, simulated calibration curves were generated for idealized 100% ortho-para methylene-linked oligomers and for 100% para-para-linked oligomers.

GPC chromatograms for a series of commercial novolacs, including resins with statistical distributions of ortho and para linkages and high ortho novolac resins were measured. Carbon-13 NMR provided the relative compositions of ortho-ortho-, ortho-para-, and para-para-linked methylene groups. Molecular weights from GPC were calculated by considering the fractions of each type of linkage multiplied by the molecular weights calculated from each of the three ortho-ortho (experimental), ortho-para (simulated), and ortho-ortho (simulated) GPC calibration curves. Good agreement was found between the resin molecular weights measured from <sup>1</sup>H NMR and the interpolated GPC numbers for oligomers up to an average of four to five units per chain, whereas more deviation was observed for higher molecular weights. This was attributed to complicated intramolecular hydrogen bonding in the higher molecular weight materials. Another factor may be that branching becomes significant in the higher molecular weight materials and the hydrodynamic volume effects of architecture are also complicated.

Proton NMR integrations of methylene and aromatic regions can be used to calculate the number-average molecular weights of novolac resins<sup>29</sup>:

$$\frac{[\text{CH}_2]}{[\text{Ar}]} = \frac{2n - 2}{3n + 2} \quad (7.1)$$

where  $[\text{CH}_2]/[\text{Ar}]$  is the ratio of methylene protons to aromatic protons and  $n$  is the number of phenolic units. The method is quite accurate for novolacs with less than eight repeat units.

Solution <sup>13</sup>C NMR has been used extensively to examine the chemical structures of phenolic resins.<sup>23,30</sup> By ratioing the integration of peaks, degree of polymerization, number-average molecular weights, degrees of branching, numbers of free ortho and para positions, and isomer distributions have been evaluated. A typical <sup>13</sup>C NMR spectrum of a novolac resin shows three regions (Table 7.4): The methylene linkages resonate between 30 and 40 ppm; the peaks between 146 and 157 ppm are due to hydroxyl-substituted aromatic carbons; and peaks between 113 and 135 ppm represent the remainder of the aromatic carbons.

**TABLE 7.4 Peak Assignments for  $^{13}\text{C}$  NMR Chemical Shifts of Phenolic Resins<sup>a</sup>**

Chemical Shift Region (ppm)	Assignment
150–156	Hydroxyl-substituted phenolic carbons
127–135	Other phenolic carbons
121	Para-unsubstituted phenolic carbons
116	Ortho-unsubstituted phenolic carbons
85.9	HO-CH <sub>2</sub> -O-CH <sub>2</sub> -OH
81.4	HO-CH <sub>2</sub> -OH
71.1	Para-linked dimethylene ether
68.2	Ortho-linked dimethylene ether
40.8	Para–para methylene linkages
35.5	Para–ortho methylene linkages
31.5	Ortho–ortho methylene linkages

<sup>a</sup>From refs. 31 and 41.

The number of remaining ortho reactive sites versus the number of para reactive sites can also be calculated using  $^{13}\text{C}$  NMR (Table 7.4). Since the rates of novolac cure reactions differ with the amount of ortho versus para reactive sites available, it is of great interest to calculate these parameters.

Degrees of polymerization can be calculated from quantitative  $^{13}\text{C}$  NMR data by considering the number of substituted (reacted) relative to unsubstituted (not yet reacted) ortho and para phenolic carbons where  $[S]$  is the sum of substituted ortho and para carbons and  $[S] + [U]$  is the total ortho and para carbons. The fraction of reacted ortho and para sites is denoted by  $f_s$  [Eq. (7.2)]. Thus, the number-average number of phenol units per chain ( $x$ ) can be calculated using Eq. (7.3). This leads to a simple calculation of  $M_n = x \times 106 - 14$ :

$$f_s = \frac{[S]}{[S] + [U]} \quad (7.2)$$

$$x = \frac{1}{(1 - 1.5 f_s)} \quad (7.3)$$

Fourier transform infrared (FTIR) and FT Raman spectroscopy have been used to characterize phenolic compounds. The lack of hydroxyl interference is a major advantage of using FT Raman spectroscopy as opposed to FTIR to characterize phenolic compounds. Two regions of interest in Raman spectra are between 2800 and 4000  $\text{cm}^{-1}$ , where phenyl C–H stretching and methylene bridges are observed, and between 400 and 1800  $\text{cm}^{-1}$ .<sup>31</sup> For a high-ortho novolac resin, the phenyl C–H stretch and methylene bridge appear at 3060 and 2940  $\text{cm}^{-1}$ , respectively. In the fingerprint region, the main bands are 1430–1470  $\text{cm}^{-1}$  representative of methylene linkages and 600–950  $\text{cm}^{-1}$  for out-of-plane phenyl

C–H bonds. Phenol, mono-ortho, and di- and tri-substituted phenolic rings can be monitored between 814–831, 753–794, 820–855, and 912–917  $\text{cm}^{-1}$ , respectively. Para-substituted phenolic rings also absorb in the 820–855- $\text{cm}^{-1}$  region.

Mandal and Hay<sup>28</sup> used MALDI–TOF mass spectrometry to determine the absolute molecular masses and endgroups of 4-phenylphenol novolac resins prepared in xylene or chlorobenzene. Peaks with a mass difference of 44 (the molecular weight of a xylene endgroup) suggested that reactions conducted in xylene included some incorporation of xylene onto the chain ends when a strong acid such as sulfuric acid was used to catalyze the reaction. By contrast, no xylene was reacted into the chain when a milder acid catalyst such as oxalic acid was used. No chlorobenzene was incorporated regardless of the catalyst used.

### 7.3.7 Hydrogen Bonding

The abundant hydroxyl groups on phenolic resins cause these materials to form strong intra- and intermolecular hydrogen bonds. Intramolecular hydrogen bonding of phenolic resins gives rise to their hyperacidity while intermolecular hydrogen bonding facilitates miscibility with a number of materials containing electron donors such as carbonyl, amide, hydroxyl, ether, and ester groups. Miscible polymer blends of novolac resins include those with some polyamides,<sup>32</sup> poly(ethylene oxide),<sup>33</sup> poly(hydroxyether)s,<sup>34</sup> poly(vinyl alcohol),<sup>35</sup> and poly(decamethylene adipate) and other poly(adipate ester)s.<sup>36</sup> The specific strength of hydrogen bonding is a function of the groups involved; for example, hydroxyl–hydroxyl interactions are stronger than hydroxyl–ether interactions.<sup>37</sup>

The effects of intermolecular hydrogen bonding on neat novolac resins with compounds containing hydrogen acceptors (e.g., 1,4-diazabicyclo[2,2,2]octane (DABCO) and hexamethylene tetramine) were also investigated.<sup>38</sup> Glass transition temperatures of neat resins and blends were measured using differential scanning calorimetry (DSC) to assess the degrees of hydrogen bonding. Hydrogen-bonding interactions of novolac resins with electron donor sites such as oxygen, nitrogen, or chlorine atoms resulted in increased  $T_g$ .

The propensity for dry novolac resins to absorb water at room temperature under 100% humidity is another indication that strong hydrogen bonds form. Approximately 15 wt % water is absorbed by the novolac after 4 d, which corresponds to one water molecule per hydroxyl group.<sup>38</sup>

Dielectric measurements were used to evaluate the degrees of inter- and intramolecular hydrogen bonding in novolac resins.<sup>39</sup> The frequency dependence of complex permittivity ( $\epsilon^*$ ) within a relaxation region can be described with a Havriliak and Negami function (HN function):

$$\epsilon^* = \epsilon_\infty + \frac{\epsilon_S - \epsilon_\infty}{[1 + (i\omega\tau_0)^\beta]^\gamma} \quad (7.4)$$

where  $\epsilon_S$  and  $\epsilon_\infty$  are the relaxed and unrelaxed dielectric constants,  $\omega$  is the angular frequency,  $\tau_0$  is the relaxation time, and  $\beta$  and  $\gamma$  are fitting parameters. The complex permittivity is comprised of permittivity ( $\epsilon'$ ) and dielectric loss

( $\epsilon''$ ). Fitting parameters in the HN function are related to shape parameters  $m$  and  $n$ , which describe the limiting behavior of dielectric loss ( $\epsilon''$ ) at low and high frequencies, respectively. Intermolecular (characterized by  $m$ ) and intramolecular (characterized by  $n$ ) hydrogen bonding can be correlated with  $m$  and  $n$  values which range from 0 to 1 (where lower values correspond to stronger hydrogen bonding). For one novolac resin examined ( $M_n = 1526$  determined via GPC using polystyrene standards,  $MWD = 2.6$ ,  $T_g = 57^\circ\text{C}$ ),  $m$  was 0.52 and  $n$  was 0.2. These results were considered indicative of strong intramolecular hydrogen bonding within the novolac structures.

### 7.3.8 Novolac Crosslinking with HMTA

The most common crosslinking agent for novolac resins is HMTA which provides a source of formaldehyde. Novolac resins prepared from a phenol-formaldehyde (F/P) ratio of 1/0.8 can be cured with 8–15 wt % HMTA, although it has been reported that 9–10 wt % results in networks with the best overall performance.<sup>3</sup>

#### 7.3.8.1 Initial Reactions of Novolacs with HMTA

The initial cure reactions of a novolac with HMTA were studied by heating the reactants at  $90^\circ\text{C}$  for 6 h, then raising the temperature incrementally to a maximum of  $205^\circ\text{C}$ . This led to mostly hydroxybenzylamine and benzoxazine intermediates (Fig. 7.14).<sup>40,41</sup> Hydroxybenzylamines form via repeated electrophilic aromatic substitutions of the active phenolic ring carbons on the methylenes of the HMTA (and derivatives of HMTA). Since novolac resins form strong intermolecular hydrogen bonds with electron donors, a plausible mechanism for the initial reaction between novolac and HMTA involves hydrogen bonding between phenolic hydroxyl groups and an HMTA nitrogen (Fig. 7.14). Such hydrogen bonding can lead to a proton transfer from which a phenolate ion is generated. A negatively charged ortho or para carbon can attack the methylene carbon next to the positively charged nitrogen on HMTA, which results in cleavage of a C–N bond. Benzoxazines form by nucleophilic attack of the phenolic oxygen on HMTA-phenolic intermediates (Fig. 7.14). Upon further reaction, methylene linkages form as the major product of both types of intermediates through various thermal decomposition pathways.

Since a small amount of water is always present in novolac resins, it has also been suggested that some decomposition of HMTA proceeds by hydrolysis, leading to the elimination of formaldehyde and amino-methylol compounds (Fig. 7.15).<sup>42</sup> Phenols can react with the formaldehyde elimination product to extend the novolac chain or form methylene-bridged crosslinks. Alternatively, phenol can react with amino-methylol intermediates in combination with formaldehyde to produce ortho- or para-hydroxybenzylamines (i.e., Mannich-type reactions).

Reaction pathways involved in the curing of novolacs with HMTA have been extensively investigated by Solomon and co-workers.<sup>43–50</sup> In a series of model studies where 2,6-xyleneol and/or 2,4-xyleneol was reacted with HMTA, these workers found that the types of linkages formed were affected by the initial

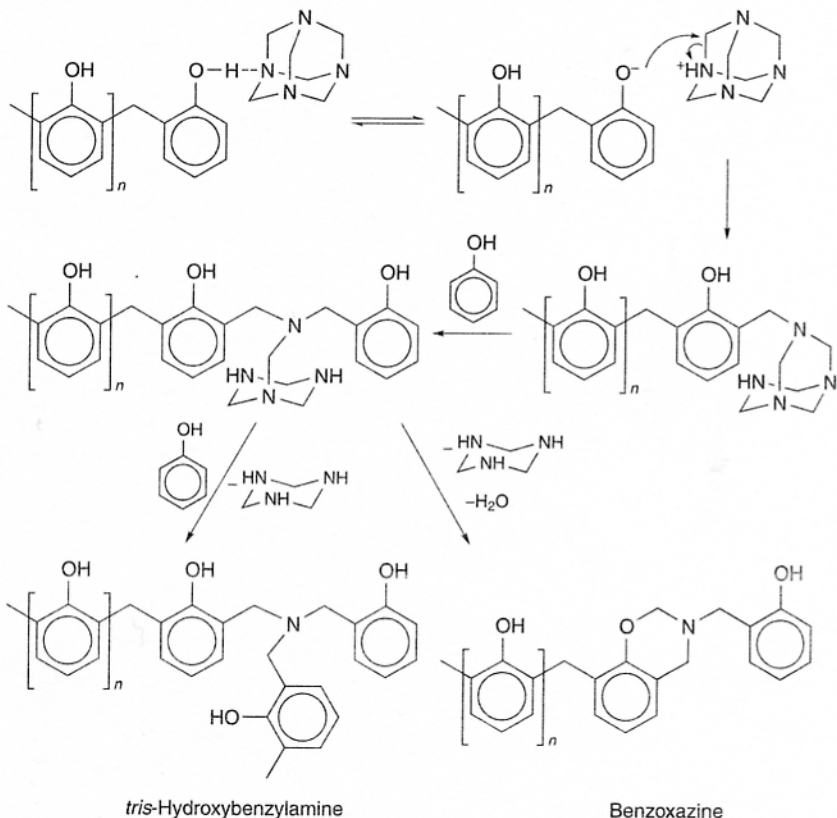


**Figure 7.14** Initial reaction of novolac and HMTA via hydrogen-bonding mechanism.

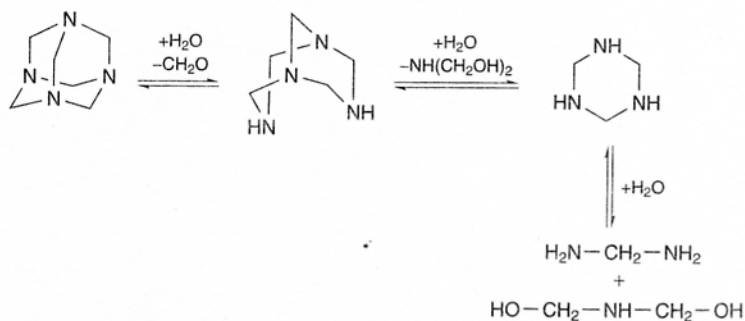


**Figure 7.15** Decomposition of HMTA.

chemical structure of the novolac, that is, amount of ortho versus para reactive positions, amount of HMTA, and pH. Reaction intermediates for the cures were identified, mostly via FTIR,  $^{13}\text{C}$  NMR, and  $^{15}\text{N}$  NMR.

As previously described, the main intermediates generated from the initial reaction between ortho reactive sites on novolac resins and HMTA are hydroxybenzylamines and benzoxazines.<sup>44</sup> Triazines, diamines, and, in the presence of trace amounts of water, benzyl alcohols and ethers also form (Fig. 7.16). Similar intermediates, with the exception of benzoxazines, are also observed when para sites react with HMTA.

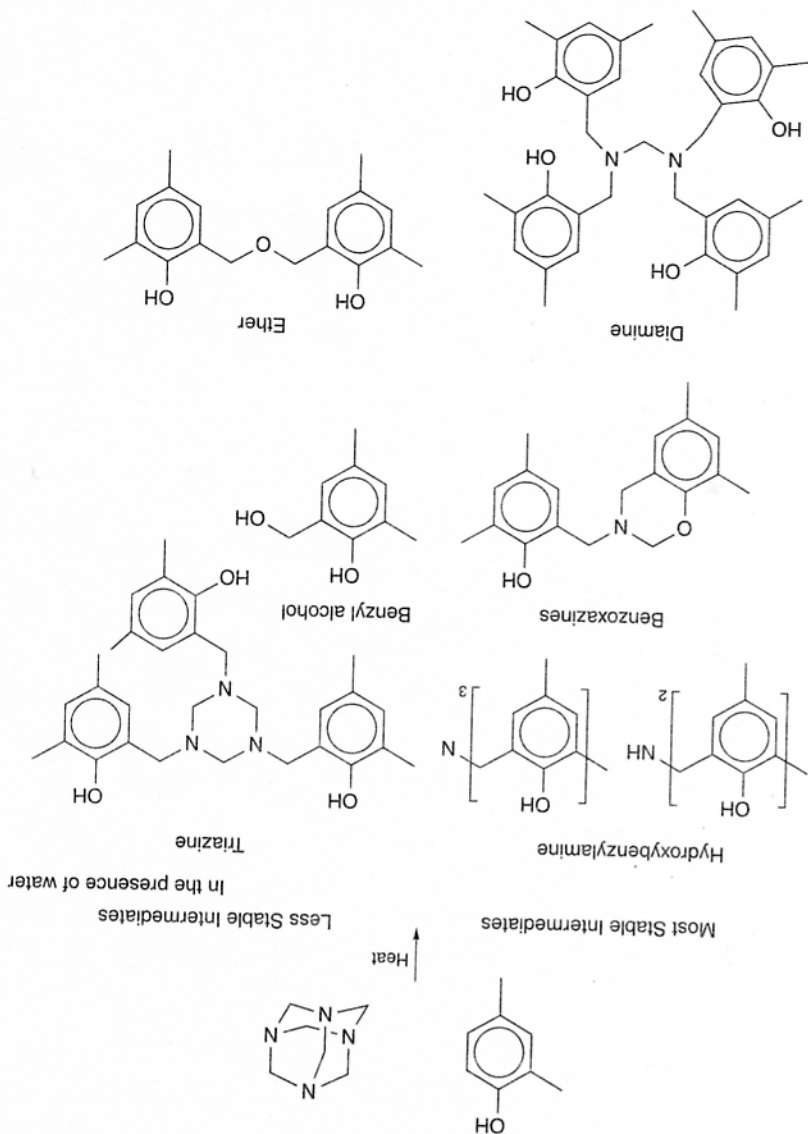


Figure 7.16 Possible reaction intermediates for the reaction of 2,4-xylenol with HMTA.

Thermolysis rates to form methylene linkages depend on the stabilities of hydroxybenzylamine and benzoxazine intermediates. Comparatively, ortho-linked hydroxybenzylamine intermediates are more stable than para-linked structures because six-membered rings can form between the nitrogen and phenolic hydroxyl groups via intramolecular hydrogen bonding. For the same reason, benzoxazines are the most stable intermediates and decompose only at higher temperatures (185°C).<sup>45</sup> If a high-ortho novolac resin is cured with HMTA, the reaction occurs at lower temperatures due to formation of relatively unstable para-linked intermediates and the amount of side products is low. If, however, a typical novolac is used, the reaction temperature must be higher to decompose the more thermally stable ortho intermediates, and the amount of nitrogen-containing side products is significantly higher.<sup>46,47</sup>

If only ortho sites are available for reaction, the amount of hydroxybenzylamine versus benzoxazine generated is largely dependent on the novolac-HMTA ratio. Hydroxybenzylamine is favored when the HMTA content is low whereas more benzoxazine is formed at higher HMTA concentrations. This is expected since only one HMTA carbon is needed per reactive ortho position in the formation of hydroxybenzylamine, but the formation of benzoxazine requires three HMTA carbons per two reactive ortho positions. The HMTA concentration therefore is one key in determining the structure of the resulting networks. Lower HMTA contents leading to more hydroxybenzylamine intermediates means that lower temperatures can be used for decomposition into methylene bridges and correspondingly lower levels of side products form under such conditions.

### 7.3.8.2 Hydroxybenzylamine and Benzoxazine Decompositions in Novolac-HMTA Cures

**THERMAL DECOMPOSITION OF HYDROXYBENZYLAMINES** Depending on the concentration of HMTA and mobility of the system, hydroxybenzylamine and benzoxazine intermediates react by a number of pathways to form crosslinked novolac networks. Trishydroxybenzylamines eliminate benzoquinone methide between 90 and 120°C to form bishydroxybenzylamines, which decompose to methylene linkages with the elimination of  $\text{CH}_2=\text{NH}$  at higher temperatures (Fig. 7.17).<sup>46</sup>

**THERMAL DECOMPOSITION OF BENZOXAZINES** Thermal decomposition of benzoxazines does not occur substantially until the temperature reaches  $\sim 160^\circ\text{C}$ . This begins with proton transfer from a phenolic hydroxyl group to a nitrogen. Cleavage of the C-O bond with water generates a tertiary hydroxymethylamine, which can eliminate formaldehyde, then  $\text{CH}_2=\text{NH}$ , to form methylene linkages (Fig. 7.18a). Alternatively, C-N bond cleavage in the benzoxazine leads to the elimination of a benzoquinone methide, which can react with phenols to primarily yield the product methylene-bridged species (Fig. 7.18b).<sup>45</sup> Further decomposition of benzoxazines can also lead to a variety of side products in small amounts.

**REACTIONS OF BENZOXAZINES WITH PHENOLS** In the presence of 2,4-xylenol, benzoxazine intermediates react at lower temperatures ( $\sim 90^\circ\text{C}$ ) to form hydroxybenzylamines (Fig. 7.19), which can then decompose to ortho-ortho methylene

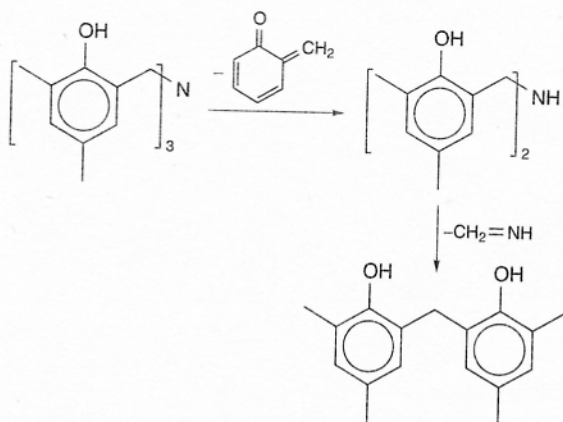


Figure 7.17 Thermal decomposition of hydroxybenzylamine.

linkages (as described in Fig. 7.17).<sup>46</sup> The reaction between benzoxazine and free ortho reactive positions on 2,4-xylenol occurs via electrophilic aromatic substitution facilitated by hydrogen bonding between benzoxazine oxygen and phenolic hydroxyl groups (Fig. 7.19).

The reaction of benzoxazine in the presence of 2,6-xylenol does not occur until  $\sim 135^{\circ}\text{C}$ , presumably because the hydrogen-bonded intermediate depicted for the 2,4-xylenol reaction (Fig. 7.19) cannot occur. All three types of linkages are obtained in this case. Para-para methylene-linked 2,6-xylenol dimers, obtained from the reaction of 2,6-xylenol with formaldehyde, formed in the decomposition of the benzoxazine (or with other by-products of that process) dominate. Possible side products from benzoxazine decomposition include formaldehyde and  $\text{CH}_2=\text{NH}$ , either of which may provide the source of methylene linkages. The amount of ortho-para linkages formed by reaction of 2,6-xylenol with benzoxazine is low. Ortho-ortho methylene-linked products presumably form by a decomposition pathway from benzoxazine (as in Fig. 7.18).

**HMTA CROSSLINKING REACTIONS OF NOVOLACS CONTAINING BOTH ORTHO AND PARA REACTIVE SITES** When both ortho and para positions on novolac materials are available for reaction with HMTA, ortho-ortho, ortho-para, and para-para methylene linkages form through several pathways. This section will address crosslinking reaction pathways in which components that have been eliminated as "by-products" reenter the reactions. In particular, reactions of quinone methides, formaldehyde, and imine will be discussed. We will also describe exchange reactions between hydroxybenzylamine intermediates with phenolic methylol derivatives which lead to methylene-bridged final products. Exchange reactions between two different hydroxybenzylamine intermediates, which lead to primarily ortho-ortho-linked products, are also important.

In one model reaction where tris(para-hydroxybenzyl)amine was heated to  $205^{\circ}\text{C}$  in the presence of 2,4-xylenol (1 : 1 ratio), the ortho-ortho, ortho-para,

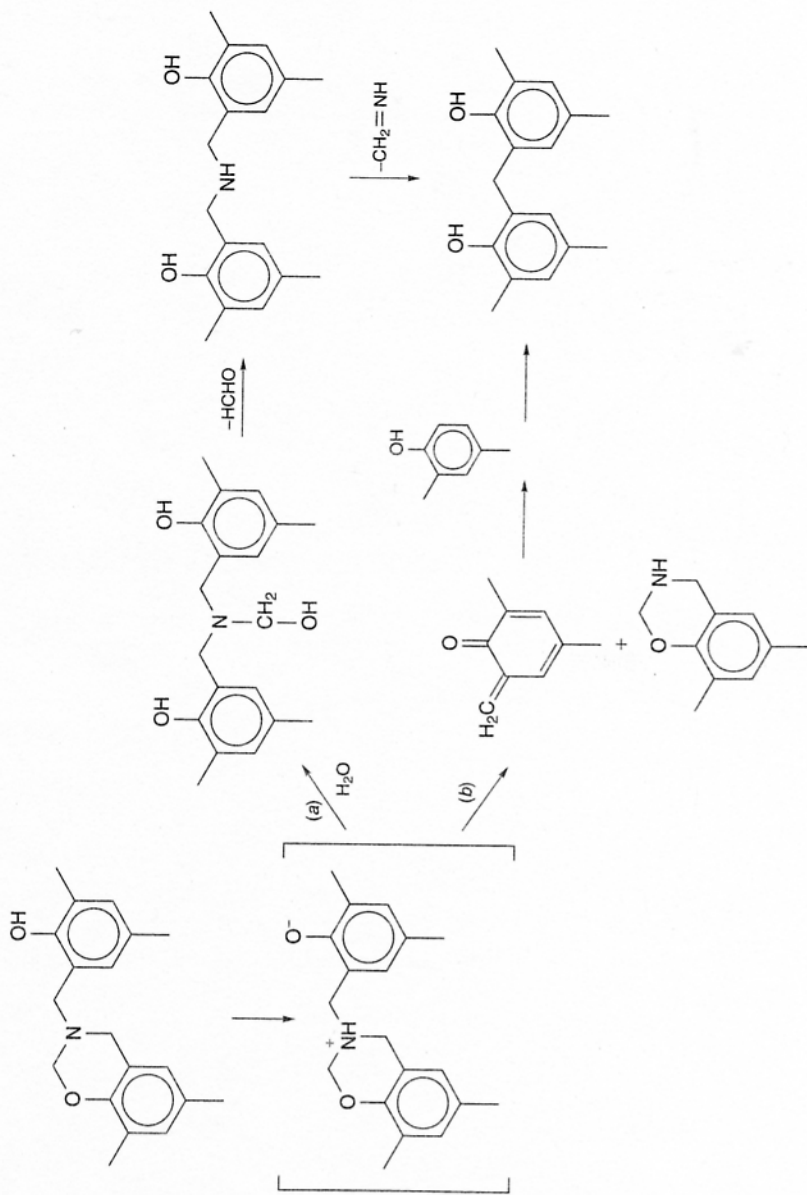


Figure 7.18 Thermal decomposition of benzoxazine.

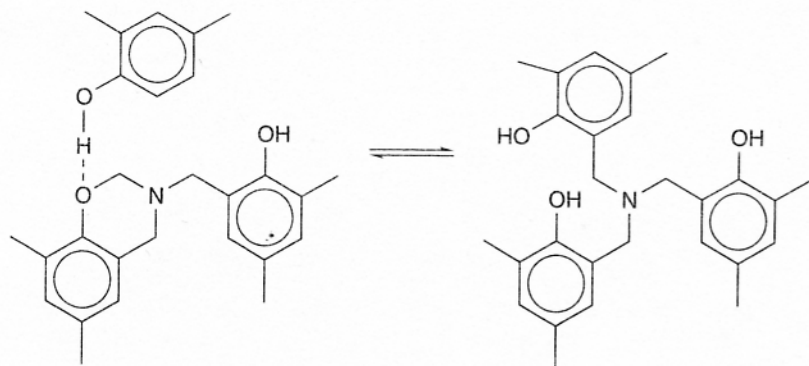
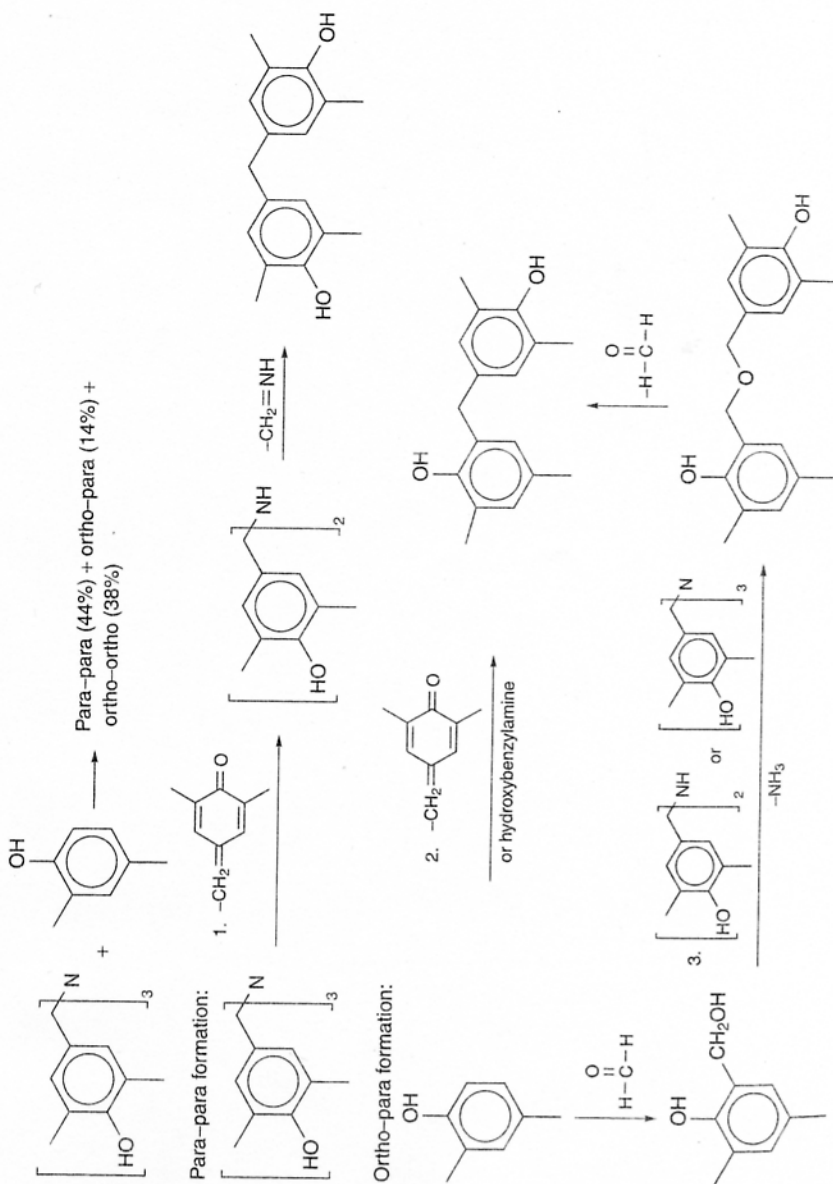


Figure 7.19 Reaction of benzoxazines and 2,4-xylenol.

and para-para methylene bridge ratios in the products were found to be 44, 14, and 38%, respectively (Fig. 7.20).<sup>48</sup> This model study demonstrated the importance of benzoquinone methide intermediates in the formation of various products in the novolac-HMTA curing reaction. Formaldehyde,  $\text{CH}_2=\text{NH}$ , and water liberated during the cure reaction also affect the reaction pathways (pathways 3, 4, and 5). Approximately 4% of 1,2-bis(para-hydroxyphenyl)ethane was also observed, presumably formed through dimerization of two quinone methides.

Para-para methylene linkages appeared first via hydroxybenzylamine decomposition at lower temperatures (pathway 1 in Fig. 7.20). Ortho-para methylene linkages also formed at the lower reaction temperatures (pathway 2). Since the only source of an ortho methylene-linked phenol product was the 2,4-xylenol starting material, these mixed products must have formed by the reaction of 2,4-xylenol with either a para-hydroxybenzylamine or with a quinone methide eliminated in pathway 1. Ortho-para methylene linkages also formed at higher reaction temperatures, which were attributed to exchange reactions between a methylol derivative of 2,4-xylenol and a hydroxybenzylamine (pathway 3). Ortho-ortho methylene linkages formed only at higher temperatures via hydroxybenzylamine exchange and methylol dimerization reactions described in pathways 4 and 5. The reactions depicted in pathway 4 involved sequential exchanges between para- and ortho-substituted intermediates through nucleophilic substitutions on hydroxybenzylamines. Since the amount of ortho-para-linked products was low, it was suggested that the major product of pathway 4 was the ortho-ortho linkage. This is reasonable since the equilibrium of these exchange reactions lies toward ortho-hydroxybenzylamines where hydrogen bonding provides stability. These more thermally stable hydroxybenzylamines then decompose at higher temperatures to form ortho-ortho linkages.

Small amounts of various phenolic side products that incorporate groups such as imines, amides, ethers, and ethanes into the networks also form. A number of these side products undergo further reactions which eventually lead to methylene linkages. Some side products generally remain in the networks even after heating at 205°C.





Lim et al. also investigated HMTA-phenolic reactions with somewhat larger model compounds (e.g., two- and four-ring compounds) and established that similar reaction pathways to those described previously occurred.<sup>50</sup> For these model compounds (as opposed to one-ring model compounds), which are more representative of typical oligomeric systems, increased molecular weight favored the formation of hydroxybenzylamines but not benzoxazines. This was suggested to be a steric effect.

Other crosslinking agents that provide sources of formaldehyde for methylene linkages include paraformaldehyde and trioxane, but these have only achieved limited importance. Quantitative <sup>13</sup>C solid-state NMR and FT Raman spectroscopy were used to monitor the cure reactions of a high-ortho novolac resin using paraformaldehyde under different conditions.<sup>31</sup> The weight percent paraformaldehyde needed to achieve the maximum crosslinking (1.5 mol formaldehyde/mol phenol) for the particular novolac examined ( $M_n = 430$  g/mol determined via <sup>13</sup>C NMR) was calculated to be 17.76 wt %. Eleven weight percent formaldehyde was used in these studies so that phenol sites were in excess. The degree of conversion was assessed by comparing the formaldehyde-to-phenol ratio in the polymer to 1.18. As expected, higher temperatures and/or pressures lead to higher reaction conversions. However, none of these reaction conversions reached 100%, and this was attributed to a lack of mobility.

## 7.4 RESOLE RESINS AND NETWORKS

### 7.4.1 Resole Resin Syntheses

Resoles are prepared under alkaline conditions using an excess of formaldehyde over phenol (1 : 1 to 3 : 1) at typical temperatures of 60–80°C. The basic catalysts commonly used are NaOH, Na<sub>2</sub>CO<sub>3</sub>, KOH, K<sub>2</sub>CO<sub>3</sub>, Ba(OH)<sub>2</sub>, R<sub>4</sub>NOH, NH<sub>3</sub>, RNH<sub>2</sub>, and R<sub>2</sub>NH.<sup>4</sup> In aqueous solutions, ammonia and HMTA are easily hydrolyzed to amines and also catalyze resole syntheses. Typical resole resins comprise a mixture of monomers, dimers, trimers, and small amounts of higher molecular weight oligomers with multiple methylol functional groups.

Resole syntheses entail substitution of formaldehyde (or formaldehyde derivatives) on phenolic ortho and para positions followed by methylol condensation reactions which form dimers and oligomers. Under basic conditions, phenolate rings are the reactive species for electrophilic aromatic substitution reactions. A simplified mechanism is generally used to depict the formaldehyde substitution on the phenol rings (Fig. 7.21). It should be noted that this mechanism does not account for pH effects, the type of catalyst, or the formation of hemiformals. Mixtures of mono-, di-, and trihydroxymethyl-substituted phenols are produced.

Phenol reacts with formaldehyde in either the ortho or the para position to form monohydroxymethyl-substituted phenols, which further react with formaldehyde to form di- and trihydroxymethyl-substituted phenols (Fig. 7.22).

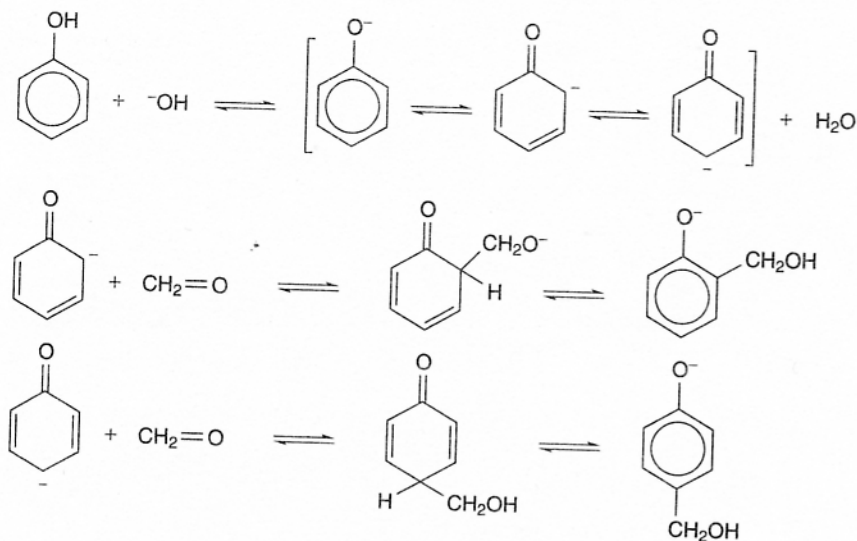


Figure 7.21 Mechanism of resole synthesis.

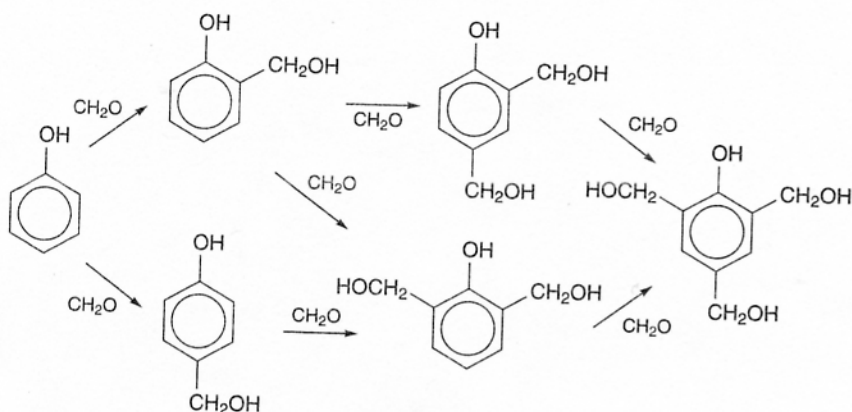


Figure 7.22 Reaction pathways for phenol-formaldehyde reactions under alkaline conditions.

Condensation reactions between two hydroxymethyl substituents eliminate water to form ether linkages (Fig. 7.23a) or eliminate both water and formaldehyde to form methylene linkages (Fig. 7.23b). Ether formation is favored under neutral or acidic conditions and up to  $\sim 130^\circ\text{C}$  above which formaldehyde departs and methylene linkages are generated. The methylene linkage formation reaction, which eliminates water and formaldehyde, is more prevalent under basic conditions. Condensation reactions between hydroxymethyl groups and reactive

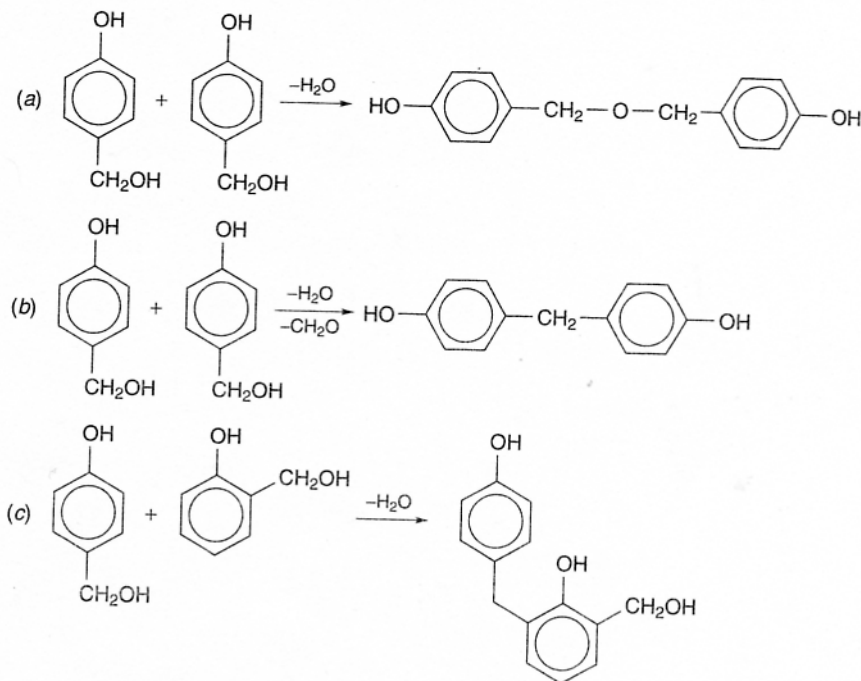


Figure 7.23 Condensation of hydroxymethyl groups.

ortho or para ring positions also lead to methylene bridges between phenolic rings (Fig. 7.23c). Relative reactivities of hydroxymethyl-substituted phenols with formaldehyde and with other hydroxymethyl-substituted phenols appear to be strongly dependent on interactions between ortho-methylol groups and the phenolic hydroxyl position. Hydroxymethyl condensation reactions under basic conditions strongly favor the formation of para-para and ortho-para methylene linkages.

Quinone methides are the key intermediates in both resole resin syntheses and crosslinking reactions. They form by the dehydration of hydroxymethylphenols or dimethylether linkages (Fig. 7.24). Resonance forms for quinone methides include both quinoid and benzoid structures (Fig. 7.25). The oligomerization or crosslinking reaction proceeds by nucleophilic attack on the quinone methide carbon.

The ortho-quinone methides are difficult to isolate due to their high reactivity, which leads to rapid Diels-Alder dimerization or trimerization (Fig. 7.26). At 150°C, a partial retro-Diels-Alder reaction of the trimer can occur to form ortho-quinone methide and bis(2-hydroxy-3,5-dimethylphenyl) ethane (dimer).<sup>51</sup>

Base-catalyzed phenol-formaldehyde reactions exhibit second-order kinetics [Eq. (5)]. Several alkylphenols such as cresols also follow this rate equation:

$$\text{Rate} = k[\text{phenolate}][\text{formaldehyde}] \quad (7.5)$$

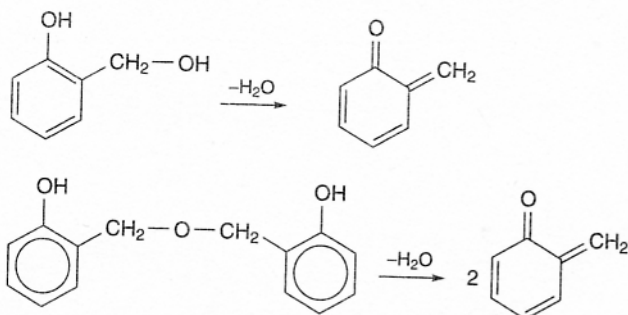


Figure 7.24 Dehydration of methylols or benzylic ethers to form quinone methides.

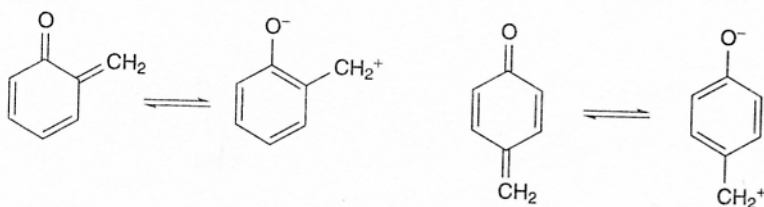


Figure 7.25 Resonance of quinone methides.

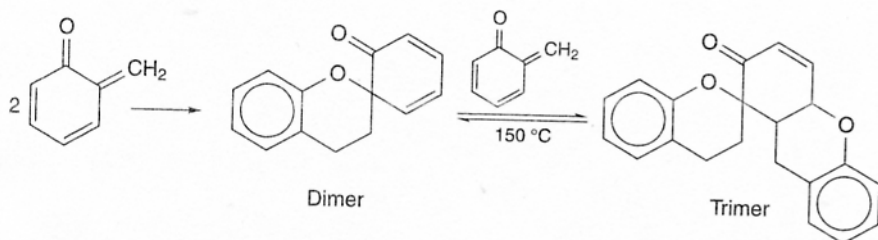


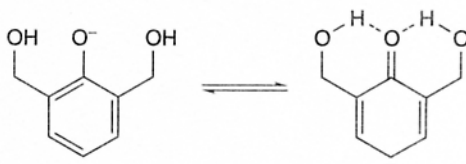
Figure 7.26 Dimer and trimer structures of ortho-quinone methides.

The rate constants for various hydroxymethylation steps (Fig. 7.22) have been evaluated by several groups (Table 7.5)<sup>52-54</sup> and more recently by Grenier-Loustalot et al.<sup>56</sup>

Some consensus observations for reactions conducted at  $30^\circ\text{C}$  indicate that the para reactive site on phenol is slightly more reactive than ortho reactive sites due to higher electron density on the para position. In addition, ortho-hydroxymethyl substituents significantly activate the rings toward further electrophilic addition of formaldehyde. This is especially pronounced for 2,6-dihydroxymethylphenols. The ortho-hydroxymethyl substituents are proposed to stabilize the quinoid resonance form via hydrogen bonding between the phenolic hydroxyl and ortho-hydroxymethyl groups in basic aqueous media (Fig. 7.27). This intramolecular stabilization activates the para position by intensifying electron density on the

**TABLE 7.5** Relative Positional Reaction Rates in Base-Catalyzed Phenol-Formaldehyde Reaction

	Relative Reaction Rates		
	Reference 52	Reference 53	Reference 54
Phenol → 2-hydroxymethylphenol	1.00	1.00	1.00
Phenol → 4-hydroxymethylphenol	1.18	1.09	1.46
2-Hydroxymethylphenol → 2,6-dihydroxymethylphenol	1.66	1.98	1.75
2-Hydroxymethylphenol → 2,4-dihydroxymethylphenol	1.39	1.80	3.05
4-Hydroxymethylphenol → 2,4-dihydroxymethylphenol	0.71	0.79	0.85
2,4-Dihydroxymethylphenol → 2,4,6-trihydroxymethylphenol	1.73	1.67	2.04
2,6-Dihydroxymethylphenol → 2,4,6-trihydroxymethylphenol	7.94	3.33	4.36

**Figure 7.27** Quinoid resonance forms activating the para ring position.

para carbon. This reasoning, however, does not explain the reduced reactivity reported for 2,4-dihydroxymethylphenol.

More recently, the reaction advancement of resole syntheses (pH = 8 and 60°C) was monitored using high-performance liquid chromatography (HPLC), <sup>13</sup>C NMR, and chemical assays.<sup>55,56</sup> The disappearance of phenol and the appearances of various hydroxymethyl-substituted phenolic monomers and dimers have been measured. By assessing the residual monomer as a function of reaction time, this work also demonstrated the unusually high reactivity of 2,6-dihydroxymethylphenol. The rate constants for phenolic monomers toward formaldehyde substitution have been measured (Table 7.6).

As the reactions proceed, the disappearance of phenol is delayed due to competition for reaction with formaldehyde between phenol and the faster reacting hydroxymethyl-substituted phenols. Competition also exists between formaldehyde substitution reactions and condensation reactions between rings. Condensation reactions between two ortho-hydroxymethyl substituents are the least favorable condensation pathway. Depending on the reaction conditions, substitutions occur

**TABLE 7.6** Second-Order Rate Constants for Reaction of Phenolic Monomers with Formaldehyde<sup>a</sup>

Compound	$k$ (mol <sup>-1</sup> ·h <sup>-1</sup> ) × 10 <sup>2</sup>
Phenol	5.1
2-Hydroxymethylphenol	9.9
4-Hydroxymethylphenol	10.7
2,4-Dihydroxymethylphenol	8.6
2,6-Dihydroxymethylphenol	13.0

<sup>a</sup>From Ref. 56.

predominately in the earlier stages of reaction, and condensations become the major reactions in later stages.<sup>55</sup>

As described previously, condensation reactions of hydroxymethyl substituents strongly favor the formation of para-para and ortho-para linkages.<sup>57-59</sup> Various hydroxymethyl-substituted phenolic monomers were heated in the absence of formaldehyde (60°C, pH = 8.0) to investigate condensation reactions under typical resole synthesis conditions but without formaldehyde substitution.<sup>58</sup> Only methylene linkages were observed under the basic experimental conditions. Highly substituted dimers were predominant in the product mixture since monomers with more hydroxymethyl substituents had higher probabilities for condensation. The ortho-hydroxymethyl groups only condensed with substituents in the para position, and therefore no ortho-ortho methylene linkages were observed. The para-hydroxymethyl substituents, on the other hand, reacted with either ortho- or para-hydroxymethyl substituents or reactive ring positions, but preferentially with para-hydroxymethyl groups. Carbon-13 and <sup>1</sup>H NMR monitoring condensation reactions of resole resins comprised of two to five phenolic units showed that, with the exception of one trimer containing a dimethylene ether linkage, only para-para and ortho-para methylene linkages formed.

Upon further reaction, especially at higher temperatures (70-100°C), hydroxymethylated compounds reacted to form almost exclusively para-para and ortho-para methylene linkages. Since the key intermediates for the condensation of hydroxymethylphenols are quinone methides, the formation of para-para and ortho-para methylene linkages is attributed to the exclusive formation of para-quinone methide intermediates (Fig. 7.28).<sup>5</sup> This is attributed to intramolecular hydrogen bonding of both *ortho*-hydroxymethyl substituents with the quinone methide oxygen, which lead to stable para-quinone methide structures. The para-quinone methide intermediates then react with ortho or para reactive positions to form ortho-para and para-para methylene linkages or the quinone methide reacts with hydroxymethyl groups to form ethers, which further advance to methylene linkages.

The mechanisms for model condensation reactions of para-hydroxymethyl-substituted phenol (and therefore para-quinone methide) with reactive ortho positions are described in Fig. 7.29. The phenolate derivatives react with para-quinone

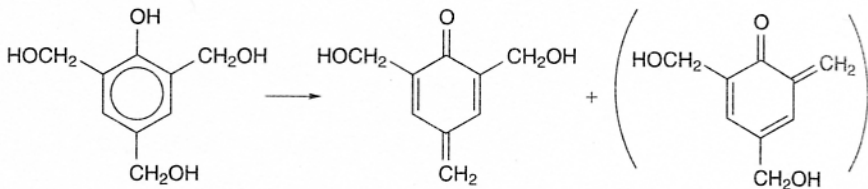


Figure 7.28 Preferential formation of para-quinone methides.

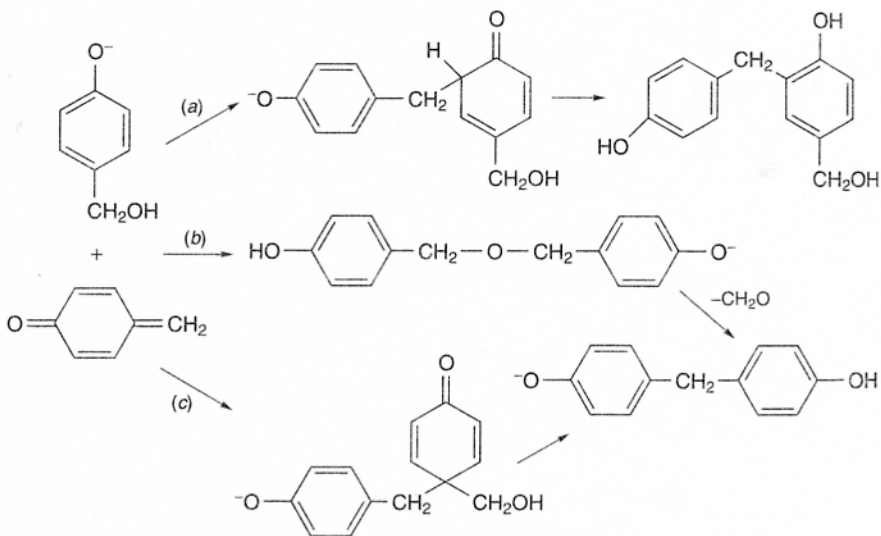


Figure 7.29 Reactions of a quinone methide with a hydroxymethyl-substituted phenolate.

methide via a Michael-type addition to form methylene linkages (Fig. 7.29a). Hydroxyl groups on methanol can also attack methide carbons to form dibenzyl ether linkages which subsequently eliminate formaldehyde to form methylene links (Fig. 7.29b). An *ipso* substitution in which a nucleophilic ring carbon having a hydroxymethyl substituent attacks a quinone methide has also been postulated to generate methylene linkages (Fig. 7.29c).

The reaction conditions, formaldehyde-to-phenol ratios, and concentration and type of catalyst govern the mechanisms and kinetics of resole syntheses. Higher formaldehyde-to-phenol ratios accelerate the reaction rates. This is to be expected since phenol-formaldehyde reactions follow second-order kinetics. Increased hydroxymethyl substitution on phenols due to higher formaldehyde compositions also leads to more condensation products.<sup>55</sup>

The amount of catalyst and pH of the reaction determine the extent of phenolate formation. Phenol-formaldehyde mixtures (F/P = 1.5, 60°C) did not react at pH = 5.5 and reaction rate increased as the pH was increased to about 9.25.<sup>55</sup>

There was a linear relationship between the rate constant and the  $[\text{NaOH}]$ -[phenol] ratio (pH between 5.5 and 9.25). It was suggested that a limiting pH of approximately 9 exists, above which an increase in pH does not enhance the rate of reaction due to saturation of phenolate anions. Considerable Canizarro side reactions occurred on formaldehyde at  $\text{pH} > 10$ .<sup>55,60</sup>

The type of catalyst influences the rate and reaction mechanism. Reactions catalyzed with both monovalent and divalent metal hydroxides,  $\text{KOH}$ ,  $\text{NaOH}$ ,  $\text{LiOH}$  and  $\text{Ba}(\text{OH})_2$ ,  $\text{Ca}(\text{OH})_2$ , and  $\text{Mg}(\text{OH})_2$ , showed that both valence and ionic radius of hydrated cations affect the formation rate and final concentrations of various reaction intermediates and products.<sup>61</sup> For the same valence, a linear relationship was observed between the formaldehyde disappearance rate and ionic radius of hydrated cations where larger cation radii gave rise to higher rate constants. In addition, irrespective of the ionic radii, divalent cations lead to faster formaldehyde disappearance rates than monovalent cations. For the proposed mechanism where an intermediate chelate participates in the reaction (Fig. 7.30), an increase in positive charge density in smaller cations was suggested to improve the stability of the chelate complex and, therefore, decrease the rate of the reaction. The radii and valence also affect the formation and disappearance of various hydroxymethylated phenolic compounds which dictate the composition of final products.

Tetraalkylammonium hydroxides have slightly lower catalytic activities than  $\text{NaOH}$  in resole syntheses. Increased alkyl length on tetraalkylammonium ions (larger ionic radii) decreased the catalytic activity. Contrary to the chelating effect, the reduced activity observed with tetraalkylammonium hydroxides was attributed to the screening effects of alkyl groups. Water solubility was limited to resole resins prepared with tetramethylammonium hydroxide and tetraethylammonium hydroxide. These catalysts also give rise to resins with longer gelation times.

Resole syntheses catalyzed with various amounts of triethylamine (pH adjusted to 8 using  $\text{NaOH}$ ) and at various pH (8.0, 8.23, and 8.36) were monitored.<sup>62</sup> As

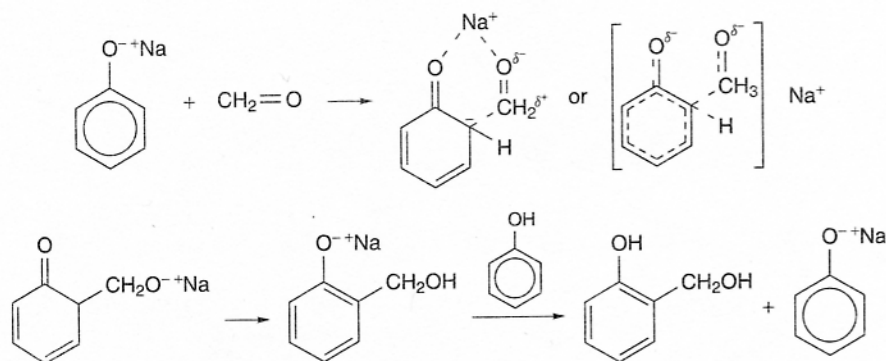


**Figure 7.30** Mechanism of phenol and formaldehyde reaction using base catalyst involving the formation of chelate.

expected, shorter condensation times, faster reaction rates, and higher advancement in polymerizations were reached with increased catalyst concentrations. The pH, on the other hand, did not affect these parameters significantly. The reaction mechanisms differed when NaOH was used to adjust the pH since the hydroxide formed phenolate ions which favored para addition reactions. In the absence of NaOH, free phenolic hydroxyl groups formed complexes with triethylamine to promote ortho substitution.

#### 7.4.2 Crosslinking Reactions of Resole Resins

Resole resins are generally crosslinked under neutral conditions between 130 and 200°C or in the presence of an acid catalyst such as hydrochloric acid, phosphoric acid, *p*-toluenesulfonic acid, and phenolsulfonic acid under ambient conditions.<sup>3</sup> The mechanisms for crosslinking under acidic conditions are similar to acid-catalyzed novolac formation. Quinone methides are the key reaction intermediates. Further condensation reactions in resole resin syntheses under basic conditions at elevated temperatures also lead to crosslinking.

The self-condensation of ortho-hydroxymethyl substituents and the condensation between this substituent with ortho or para reactive sites were investigated under neutral conditions.<sup>51</sup> 2-Hydroxymethyl-4,6-dimethylphenol was reacted (1) alone, (2) in the presence of 2,4-xyleneol, and (3) in the presence of 2,6-xyleneol. The rates of methylene versus dimethylether formation between rings at 120°C were monitored as a function of time and the percent yields after 5 h were recorded (Table 7.7). The ether linkage was more prevalent in the self-condensation of 2-hydroxymethyl-4,6-dimethylphenol. Possibly the 5% methylene-bridged product formed via the *ipso* substitution of an ortho-quinone methide electrophile onto the methylene position of another ring. Essentially no differences in product composition were observed between the 2-hydroxymethyl-4,6-dimethylphenol self-condensation and reaction of this compound in the presence of 2,6-xyleneol. The formation of methylene linkages proceeded much more favorably in the presence of 2,4-xyleneol. Moreover, increases in 2,4-xyleneol concentrations further increased the methylene linkage yield. This suggests vacant ortho

**TABLE 7.7** Percent Yield of Methylene and Ether Linkages of 2-Hydroxymethyl-4,6-Dimethylphenol Self-reaction, 1 : 1 with 2,4-Xyleneol, and 1 : 1 with 2,6-Xyleneol

	Percent Yield	
	Methylene	Ether
Self-reaction	5	80
With 2,4-xyleneol	38	65
With 2,6-xyleneol	5	80

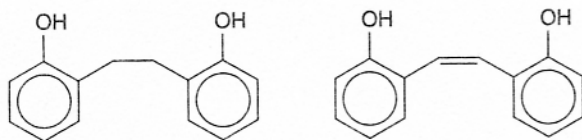


Figure 7.31 Ethane and ethene linkages derived from quinone methide structures.

positions are significantly more reactive than para reactive sites in reactions with ortho-quinone methide. These model reactions provide further evidence supporting quinone methides as the key reactive intermediates.

In addition to methylene and dimethylether linkages, cured networks contain ethane and ethene linkages (Fig. 7.31). These side products are proposed to form through quinone methide intermediates.

Crosslinking resoles in the presence of sodium carbonate or potassium carbonate lead to preferential formation of ortho-ortho methylene linkages.<sup>63</sup> Resole networks crosslinked under basic conditions showed that crosslink density depends on the degree of hydroxymethyl substitution, which is affected by the formaldehyde-to-phenol ratio, the reaction time, and the type and concentration of catalyst (uncatalyzed, with 2% NaOH, with 5% NaOH).<sup>64</sup> As expected, NaOH accelerated the rates of both hydroxymethyl substitution and methylene ether formation. Significant rate increases were observed for ortho substitutions as the amount of NaOH increased. The para substitution, which does not occur in the absence of the catalyst, formed only in small amounts in the presence of NaOH.

### 7.4.3 Resole Characterization

A number of analytical techniques such as FTIR spectroscopy,<sup>65,66</sup> <sup>13</sup>C NMR,<sup>67,68</sup> solid-state <sup>13</sup>C NMR,<sup>69</sup> GPC or size exclusion chromatography (SEC),<sup>67-72</sup> HPLC,<sup>73</sup> mass spectrometric analysis,<sup>74</sup> differential scanning calorimetry (DSC),<sup>67,75,76</sup> and dynamic mechanical analysis (DMA)<sup>77,78</sup> have been utilized to characterize resole syntheses and crosslinking reactions. Packed-column supercritical fluid chromatography with a negative-ion atmospheric pressure chemical ionization mass spectrometric detector has also been used to separate and characterize resoles resins.<sup>79</sup> This section provides some examples of how these techniques are used in practical applications.

Using FTIR spectroscopy, resole resin formation and cure reactions can be examined (Table 7.8). FTIR can be used to monitor the appearance and disappearance of hydroxymethyl groups and/or methylene ether linkages, ortho reactive groups, and para reactive groups for resole resin syntheses. Other useful information deduced from FTIR are the type of hydrogen bonding, that is, intra- versus intermolecular, the amount of free phenol present in the product, and the formaldehyde-phenol molar ratio. FTIR bands and patterns for various mono-, di-, and trisubstituted phenols have been identified using a series of model compounds.

TABLE 7.8 FTIR Absorption Band Assignment of Resole Resins

Wave Number ( $\text{cm}^{-1}$ )	Assignment	Nature
3350	v(CH)	Phenolic and methylol
3060	v(CH)	Aromatic
3020	v(CH)	Aromatic
2930	$v_{ip}(\text{CH}_2)$	Aliphatic
2860	$v_{op}(\text{CH}_2)$	Aliphatic
1610	v(C=C)	Benzene ring
1500	v(C=C)	Benzene ring
1470	d(CH <sub>2</sub> )	Aliphatic
1450	v(C=C)	Benzene ring
1370	$d_{ip}(\text{OH})$	Phenolic
1240	$v_{ip}(\text{C-O})$	Phenolic
1160	$d_{ip}(\text{CH})$	Aromatic
1100	$d_{ip}(\text{CH})$	Aromatic
1010	v(C-O)	Methylol
880	$d_{op}(\text{CH})$	Isolated H
820	$d_{op}(\text{CH})$	Adjacent 2H, para substituted
790	$d_{op}(\text{CH})$	Adjacent 3H
760	$d_{op}(\text{CH})$	Adjacent 4H, ortho substituted
690	$d_{op}(\text{CH})$	Adjacent 5H, phenol

<sup>a</sup>From ref. 65. Abbreviations: v = stretching, d = deformation, ip = in plane, op = out of plane.

The kinetics of resole cure reactions monitored via FTIR suggest that a diffusion mechanism dominates below 140°C. The cure above 140°C exhibits a homogeneous first-order reaction rate. The activation energy of the cure reaction was ~49.6 kJ/mole.<sup>66</sup>

Carbon-13 NMR has proven to be an extremely powerful technique for both monitoring the phenolic resin synthesis and determining the product compositions and structures. Insoluble resole networks can be examined using solid-state <sup>13</sup>C NMR which characterizes substitutions on ortho and para positions, the formation and disappearance of hydroxymethyl groups, and the formation of para-para methylene linkages. Analyses using <sup>13</sup>C NMR have shown good agreement with those obtained from FTIR.<sup>64</sup>

Various ionization methods were used to bombard phenol-formaldehyde oligomers in mass spectroscopic analysis. The molecular weights of resole resins were calculated using field desorption mass spectroscopy of acetyl-derivatized samples.<sup>74</sup> Phenol acetylation was used to enable quantitative characterization of all molecular fractions by increasing the molecular weights in increments of 42.

Dynamic DSC scans of resole resins show two distinguishable reaction peaks, which correspond to formaldehyde addition and the formation of ether and methylene bridges characterized by different activation energies. Kinetic parameters calculated using a regression analysis show good agreement with experimental values.<sup>75</sup>

DMA was used to determine the cure times and the onset of vitrification in resole cure reactions.<sup>77</sup> The time at which two tangents to the storage modulus curve intersect (near the final storage modulus plateau) was suggested to correspond to the cure times. In addition, the time to reach the peak of the  $\tan \delta$  curve was suggested to correspond to the vitrification point. As expected, higher cure temperatures reduced the cure times. DMA was also used to measure the degree of cure achieved by resole resins subsequent to their exposure to combinations of reaction time, temperature, and humidity.<sup>78</sup> The ultimate moduli increased with longer reaction times and lower initial moisture contents. The area under the  $\tan \delta$  curves during isothermal experiments was suggested to be inversely proportional to the degree of cure developed in samples prior to the measurement.

A NaOH-catalyzed resole resin, acetylated or treated with an ion exchange resin (neutralized and free of sodium), was analyzed using GPC in tetrahydrofuran (THF) solvent.<sup>80</sup> The molecular weight of the ion-exchange-treated resin, calculated by GPC using polystyrene standards, was significantly lower than that estimated for the acetylated resin. The molecular weight for the ion-exchange-treated resin calculated by <sup>1</sup>H NMR and vapor pressure osmometry (VPO) agreed with the results from GPC. The higher molecular weight observed for the acetylated resin was attributed to higher hydrodynamic volume and/or intermolecular association in acetylated samples.

#### 7.4.4 Resole Network Properties

Voids in resole networks detract from the mechanical properties. Irrespective of the curing conditions, all resole networks contain a significant amount of voids due to volatiles released during the cure reactions. The catalyst concentration in resole crosslinking reactions can lead to different pore microstructures, which influence the mechanical properties.<sup>81</sup> Resole networks cured using *p*-toluenesulfonic acid between 40 and 80°C showed that increased catalyst concentrations led to reduced average void diameters. Higher cure temperatures also resulted in reduced void diameters, although the effect was not as substantial. The same study showed that while the catalyst concentration did not affect the network  $T_g$ s, higher cure and postcure temperatures increased  $T_g$ s and reduced fracture strains.

In another exemplary study, optical microscopy revealed that the void content of resole networks ranged from 0.13 to 0.21.<sup>82</sup> Resole networks prepared from different F/P molar ratios showed comparable void size distributions. A bimodal distribution was observed for all networks, which was attributed to

thermodynamic phase separation of reaction volatiles (free phenol, formaldehyde, and water) and reaction kinetics.

The glass transition temperatures were determined from the peaks of  $\tan \delta$  curves measured using dynamic mechanical analysis for a series of resole networks (prepared with F/P molar ratios ranging from 1 to 2.5).<sup>82</sup> Networks obtained from resoles with high F/P molar ratios ( $>1.2$ ) had fairly consistent  $T_g$ s (between 240 and 260°C). The lowest  $T_g$  (190°C) was observed for networks prepared with low hydroxymethyl-substituted resoles (F/P = 1), and this was attributed to the low network crosslink densities at this ratio. The highest  $T_g$  occurred at F/P = 1.2 ( $\sim 280^\circ\text{C}$ ), but it superimposed the degradation temperatures. The width of the  $\tan \delta$  curves was used to assess the distributions of chain length as well as the crosslink densities. Networks cured with resoles having F/P ratios of 1.3 and 1.4 exhibited the highest  $T_g$ s and therefore the highest crosslink densities.

#### 7.4.5 Modified Phenol-Formaldehyde Resins

Phenol, formaldehyde, and urea have been copolymerized to achieve resins and subsequent networks with improved flame retardance and lower cost relative to phenol-formaldehyde analogues. The condensation of a phenolic methylol group with urea (Fig. 7.32) is believed to be the primary reaction under the weakly acidic conditions normally used.

Resins were prepared by cocondensing low-molecular-weight hydroxymethyl-substituted resoles with urea. The rate of the urea-methylol reaction was greatly enhanced by increased acidity in the reaction medium.<sup>83</sup> The para-methylol groups reacted faster than the ortho-methylol groups (presumably due to hydrogen-bonded ortho-methylol groups with phenol). The extent of urea incorporation depended on the F/P ratio and the resole-urea concentration. Increased urea incorporation ensued at higher urea concentrations and/or in the presence of highly hydroxymethylated resole resins (prepared from larger F/P ratios). Since the reactions were conducted under acidic conditions, the condensation of methylol and urea competes with methylol self-condensation. Increased urea compositions suppress the self-condensation reactions.

The curing process of trihydroxymethylphenol reacted with urea was monitored using torsional braid analysis.<sup>84</sup> Curing proceeded in two stages where the first stage occurred at lower temperatures and was attributed to the reaction of para-hydroxymethyl and urea groups. The second stage was due to the higher temperature reaction of ortho-hydroxymethyl and urea groups.

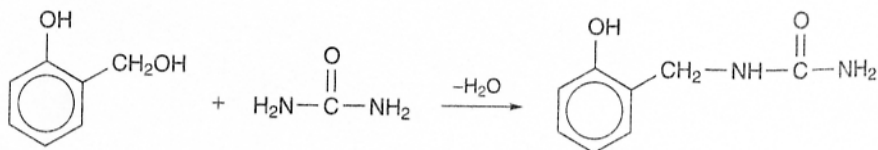


Figure 7.32 Reaction of hydroxymethylphenol and urea.

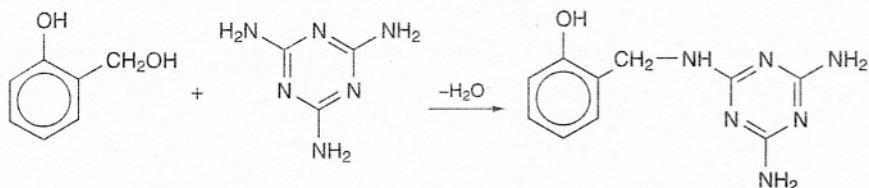


Figure 7.33 Reaction of hydroxymethylphenol and melamine.

Condensation reactions of hydroxymethyl groups on phenolic resoles and amines on melamine take place between pH 5 and 6 (Fig. 7.33). Only self-condensations of hydroxymethyl substituents occur under strongly acidic or basic conditions.

## 7.5 EPOXY-PHENOLIC NETWORKS

Void-free phenolic networks can be prepared by crosslinking novolacs with epoxies instead of HMTA. A variety of difunctional and multifunctional epoxy reagents can be used to generate networks with excellent dielectric properties.<sup>2</sup> One example of epoxy reagents used in this manner is the epoxidized novolac (Fig. 7.34) derived from the reaction of novolac oligomers with an excess of epichlorohydrin.

### 7.5.1 Mechanism of Epoxy-Phenolic Reaction

The reactions between phenolic hydroxyl groups and epoxides have been catalyzed by a variety of acid and base catalysts, group 5a compounds, and quaternary ammonium complexes,<sup>85</sup> although they are typically catalyzed by tertiary amines or phosphines, with triphenylphosphine being the most commonly used reagent. The reaction mechanism (Fig. 7.35) involves triphenylphosphine attacking an epoxide, which results in ring opening and produces a zwitterion. Rapid proton transfer occurs from the phenolic hydroxyl group to the zwitterion to form a phenoxide anion and a secondary alcohol. The phenoxide anion subsequently reacts with either an electrophilic carbon next to the phosphorus regenerating the

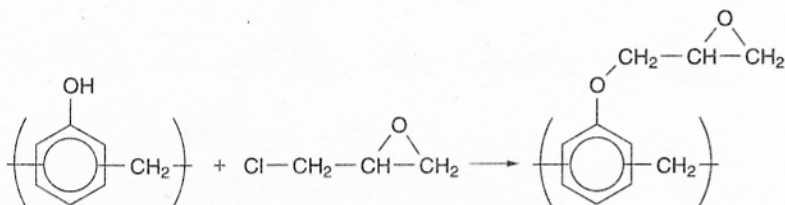


Figure 7.34 Reaction of phenol and epichlorohydrin to form epoxidized novolacs.

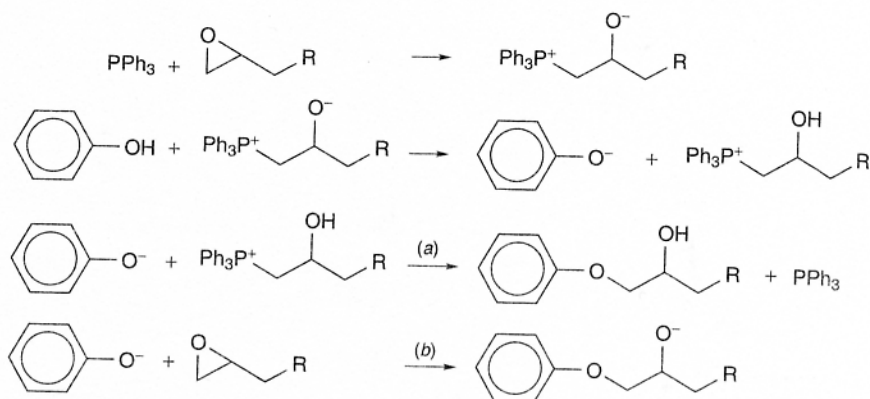


Figure 7.35 Mechanism for triphenylphosphine-catalyzed phenol-epoxy reaction.

triphenylphosphine (Fig. 7.35a)<sup>86</sup> or it can ring-open an epoxy followed by proton transfer from another phenol to regenerate the phenoxide anion (Fig. 7.35b). The phenolate anion is the reactive species for the crosslinking reaction.

Melt reaction mechanisms of tertiary aliphatic amine catalyzed phenolic-epoxy reactions were proposed to begin with a trialkylamine abstracting a phenolic hydroxyl proton to form an ion pair (Fig. 7.36). The ion pair was suggested to complex with an epoxy ring, which then dissociated to form a  $\beta$ -hydroxyether and a regenerated trialkylamine.<sup>87</sup>

Side reactions involving branching through a secondary hydroxyl group can also occur. The extent of these side reactions should decrease as the ratio of epoxy to phenol decreases since phenolate anions are significantly more nucleophilic than aliphatic hydroxyl groups.

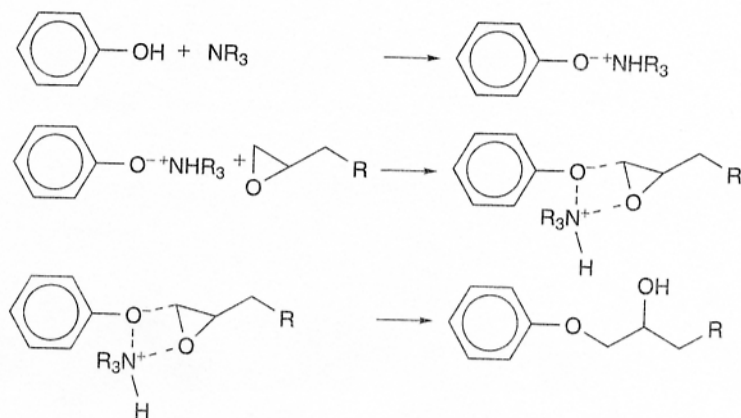


Figure 7.36 Proposed mechanism for tertiary amine-catalyzed phenol-epoxy reaction.

### 7.5.2 Epoxy-Phenolic Reaction Kinetics

A review of epoxy-novolac reaction mechanisms and kinetics is provided by Biernath et al.<sup>85</sup> Depending on the structures of the novolac and the epoxy, reactions have been reported to proceed through an  $n$ th-order mechanism or an autocatalytic mechanism.<sup>88-92</sup>

Biernath et al. concluded that phenolic novolac and epoxidized cresol novolac cure reactions using triphenylphosphine as the catalyst had a short initiation period wherein the concentration of phenolate ion increased, followed by a (steady-state) propagation regime where the number of reactive phenolate species was constant.<sup>85</sup> The epoxy ring opening was reportedly first order in the "steady-state" regime.

### 7.5.3 Epoxy-Phenol Network Properties

Void-free phenolic-epoxy networks prepared from an excess of phenolic novolac resins and various diepoxides have been investigated by Tyberg et al. (Fig. 7.37).<sup>93-95</sup> The novolacs and diepoxides were cured at approximately 200°C in the presence of triphenylphosphine and other phosphine derivatives. Network densities were controlled by stoichiometric offsets between phenol and

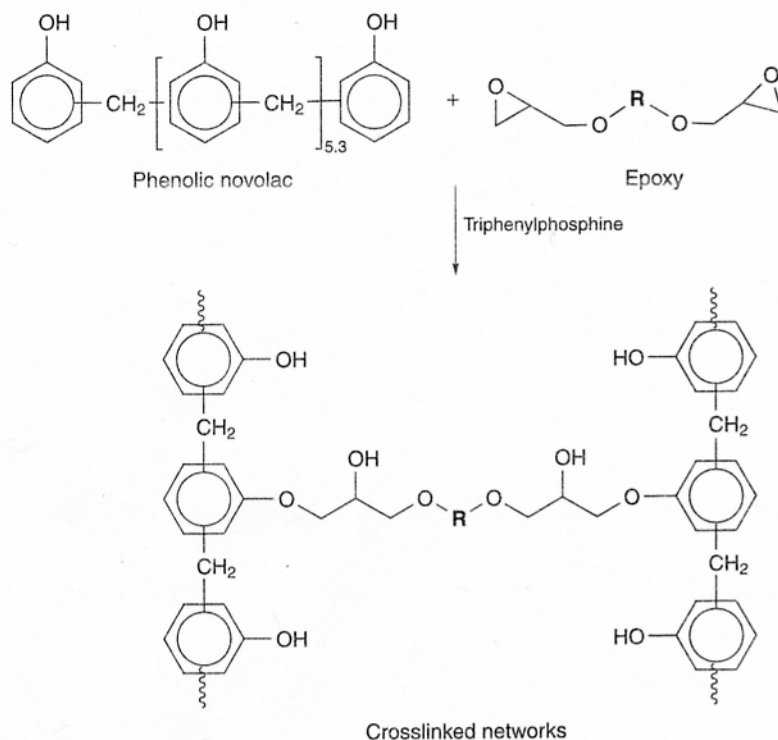


Figure 7.37 Network formation of phenolic novolac and epoxy.

epoxide groups. These networks contained high phenolic concentrations (up to ~80 wt %) to retain the high flame retardance of the phenolic materials while the mechanical properties were tailored by controlling the crosslink densities and molecular structures.

Network structure–property relationships and flame properties were determined for a novolac cured with various diepoxides (Fig. 7.38) at defined compositions. The fracture toughness of the networks, determined by the plane strain–stress intensity factors ( $K_{IC}$ ), increased with increased stoichiometric offset to a maximum of approximately  $1.0 \text{ MPa}\cdot\text{m}^{1/2}$  for the 5 phenol/1 epoxy equivalence ratio (Table 7.9). All novolac–epoxy networks were significantly tougher than a thermally cured resole network ( $0.16 \text{ MPa}\cdot\text{m}^{1/2}$ ). Further stoichiometric offset (to 7/1) reduced the fracture toughness. This was undoubtedly related to the increase in dangling ends and unconnected phenolic chains at these very high phenol-to-epoxy ratios. Likewise, as expected, glass transition temperatures of fully cured networks decreased as the distances between crosslinks ( $M_c$ ) increased.

The flame retardance was measured using a cone calorimeter with a heat flux of  $50 \text{ kW/m}^2$  and 20.95 mol %  $\text{O}_2$  content (atmospheric oxygen). All phenolic novolac–epoxy networks with relatively high novolac compositions showed much lower peak heat release rates (PHRRs) than a typical amine-cured epoxy network (bisphenol-A epoxy stoichiometrically cured with *p,p'*-diaminodiphenylsulfone) (Table 7.10). Brominated epoxy reagents were also investigated since halogenated materials are well known for their roles in promoting flame retardance. Networks cured with the brominated diepoxide showed the lowest peak heat release rates, but the char yields of these networks were lower and the smoke toxicity (CO yield/ $\text{CO}_2$  yield) was increased. Incorporating siloxane moieties into networks reduced the peak heat release rates and smoke toxicities compared to the novolac networks cured with bisphenol-A diepoxides.

A biphenyl diglycidyl ether based epoxy resin was crosslinked with amine-curing agents (4,4'-diaminodiphenylmethane and aniline novolac) and phenol-curing agents (phenol novolac and catechol novolac), and the thermomechanical

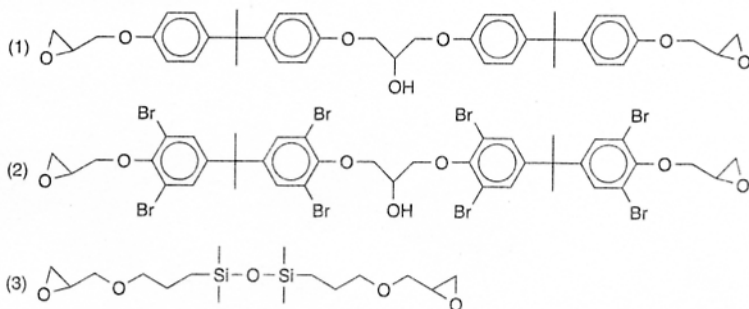


**Figure 7.38** Epoxy structures: (1) bisphenol-A-based epoxy, (2) brominated bisphenol-A-based epoxy, and (3) siloxane epoxy.

TABLE 7.9  $T_g$  and  $K_{IC}$  of Phenolic Novolac-Epoxy Networks

Epoxy	Phenol-Epoxy (wt/wt)	Phenol-Epoxy (mol/mol)	$T_g$	$K_{IC}$ (MPa·m <sup>1/2</sup> )	$M_c$ (g/mol)
Bisphenol-A epoxy cured with 4,4'-DDS	—	—	127	0.62	—
Phenolic control (thermally cured resole)	—	—	—	0.16	—
Bisphenol-A	80/20	7 : 1	114	0.70	4539
	—	5 : 1	110	1.02	—
	65/35	3 : 1	127	0.85	1413
	50/50	2 : 1	151	0.64	643
Brominated bisphenol-A	65/35	5.8 : 1	130	0.74	3511
	50/50	3.1 : 1	148	0.84	1554
Disiloxane epoxy	80/20	7.2 : 1	96	0.62	4051
	65/35	3 : 1	87	0.77	1030

TABLE 7.10 Flame Retardance of Networks Prepared from Phenolic Novolac Crosslinked with Various Epoxies

Epoxy	Phenolic-Epoxy (wt/wt)	PHRR (KW/m <sup>2</sup> )	Char Yield (%)	Smoke Toxicity <sup>a</sup> (×10 <sup>-3</sup> )
Bisphenol-A epoxy cured with 4,4'-DDS	—	1230	5	44
Phenolic control (thermally cured resole)	—	116	63	—
Bisphenol-A	80/20	260	33	27
	65/35	360	29	34
	50/50	380	23	36
Brominated bisphenol-A	65/35	165	8	189
	50/50	158	9	175
Disiloxane epoxy	80/20	226	35	15
	65/35	325	24	27

<sup>a</sup>CO/CO<sub>2</sub> release.

properties were investigated.<sup>96</sup> The presence of a distinct  $T_g$  when phenols were used to cure biphenyl-based diepoxide depended on the phenolic structure. Whereas a distinct  $T_g$  was evident in the phenolic-novolac-cured systems, no definite  $T_g$ s were observed when catechol novolac was used. The higher moduli shown by the

catechol-novolac-cured networks were attributed to the orientation of mesogenic biphenyl groups which suppressed micro-Brownian chain motions.

Network properties and microscopic structures of various epoxy resins cross-linked by phenolic novolacs were investigated by Suzuki et al.<sup>97</sup> Positron annihilation spectroscopy (PAS) was utilized to characterize intermolecular spacing of networks and the results were compared to bulk polymer properties. The lifetimes ( $\tau_3$ ) and intensities ( $I_3$ ) of the active species (positronium ions) correspond to volume and number of "holes" which constitute the free volume in the network. Networks cured with flexible epoxies had more holes throughout the temperature range, and the space increased with temperature increases. Glass transition temperatures and thermal expansion coefficients ( $\alpha$ ) were calculated from plots of  $\tau_3$  versus temperature. The  $T_g$ s and thermal expansion coefficients obtained from PAS were lower than those obtained from thermomechanical analysis. These differences were attributed to micro-Brownian motions determined by PAS versus macroscopic polymer properties determined by thermomechanical analysis.

## 7.6 BENZOXAZINES

Benzoxazines are heterocyclic compounds obtained from reaction of phenols, primary amines, and formaldehyde.<sup>98,99</sup> As described previously, they are key reaction intermediates in the HMTA-novolac cure reaction.<sup>40,43</sup> Crosslinking benzoxazine monomers at high temperatures gives rise to void-free networks with high  $T_g$ s, excellent heat resistance, good flame retardance, and low smoke toxicity.<sup>100</sup> As in HMTA-cured novolac networks, further structural rearrangement may occur at higher temperatures.

A difunctional bisphenol-A-based benzoxazine has been synthesized and characterized by GPC and <sup>1</sup>H NMR (Fig. 7.39). A small amount of dimers and oligomers also formed. Thermal crosslinking of bisphenol-A benzoxazine containing dimers and oligomers resulted in networks with relatively high  $T_g$ s. Dynamic mechanical analysis of the network showed a peak of  $\tan \delta$  at approximately 185°C.

The kinetics of bisphenol-A benzoxazine crosslinking reactions was studied using DSC.<sup>100</sup> The activation energy, estimated from plots of conversion as a function of time for different isothermal cure temperatures, was between 102 and 116 kJ/mole. Phenolic compounds with free ortho positions were suggested to initiate the benzoxazine reaction (Fig. 7.40).<sup>101</sup> Fast reactions between benzoxazines and free ortho phenolic positions, which formed hydroxybenzylamines, were facilitated by hydrogen bonding between the phenol hydroxyl and benzoxazine oxygen (as shown in Fig. 7.19). Subsequent thermal decompositions of these less stable hydroxybenzylamines led to more rapid thermal crosslinking (as described for the HMTA-novolac cure).

The reaction of bisphenol-A benzoxazine under strong and weak acidic conditions was also investigated.<sup>102</sup> The proposed mechanism for the benzoxazine ring-opening reaction in the presence of a weak acid involves an initial tautomerization between the benzoxazine ring and chain forms. In an electrophilic

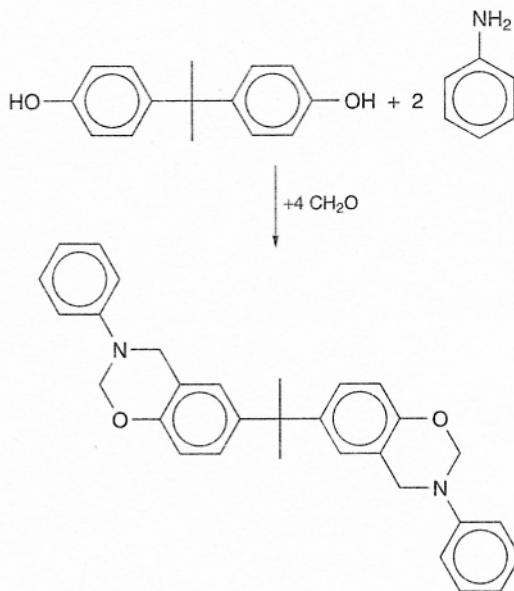


Figure 7.39 Synthesis of bisphenol-A-based benzoxazines.

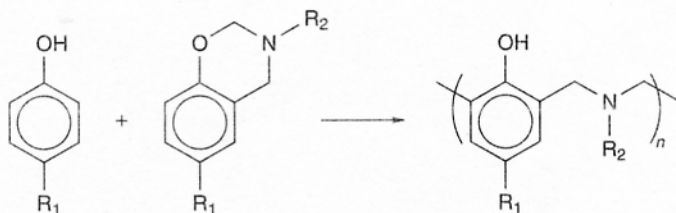


Figure 7.40 Reaction of benzoxazines with free ortho positions on phenolic compounds.

aromatic substitution reaction between a phenolic ring position and the chain tautomer, an iminium ion was suggested to follow. Strongly acidic conditions, high temperatures, and the presence of water lead to various side reactions, including benzoxazine hydrolysis in a reverse Mannich reaction. Side reactions could also terminate the reaction or lead to crosslinking.

The oxazine ring in benzoxazine assumes a distorted semichair conformation.<sup>103</sup> The ring strain and the strong basicity of the nitrogen and oxygen allow benzoxazines to undergo cationic ring-opening reactions. A number of catalysts and/or initiators such as  $\text{PCl}_5$ ,  $\text{PCl}_3$ ,  $\text{POCl}_3$ ,  $\text{TiCl}_4$ ,  $\text{AlCl}_3$ , and  $\text{MeOTf}$  are effective in promoting benzoxazine polymerization at moderate temperatures (20–50°C).<sup>104</sup> Dynamic DSC studies revealed multiple exotherms in polymerization of benzoxazine, indicating a complex reaction mechanism.

## 7.7 PHENOLIC CYANATE RESINS

Novolac hydroxyl groups reacted with cyanogen bromide under basic conditions to produce cyanate ester resins (Fig. 7.41).<sup>105,106</sup> Cyanate esters can thermally crosslink to form void-free networks, wherein at least some triazine rings form. The resultant networks possess high  $T_g$ s, high char yields at 900°C, and high decomposition temperatures.<sup>105</sup>

Novolac resins containing cardanol moieties have also been converted to cyanate ester resins.<sup>107</sup> The thermal stability and char yields, however, were reduced when cardanol was incorporated into the networks.

## 7.8 THERMAL AND THERMO-OXIDATIVE DEGRADATION

Phenolic networks are well known for their excellent thermal and thermo-oxidative stabilities. The mechanisms for high-temperature phenolic degradation include dehydration, thermal crosslinking, and oxidation, which eventually lead to char.

Thermal degradation below 300°C in inert atmospheres produces only small amounts of gaseous products. These are mostly unreacted monomers or water, which are by-products eliminated from condensation reactions between hydroxymethyl groups and reactive ortho or para positions on phenolic rings. A small

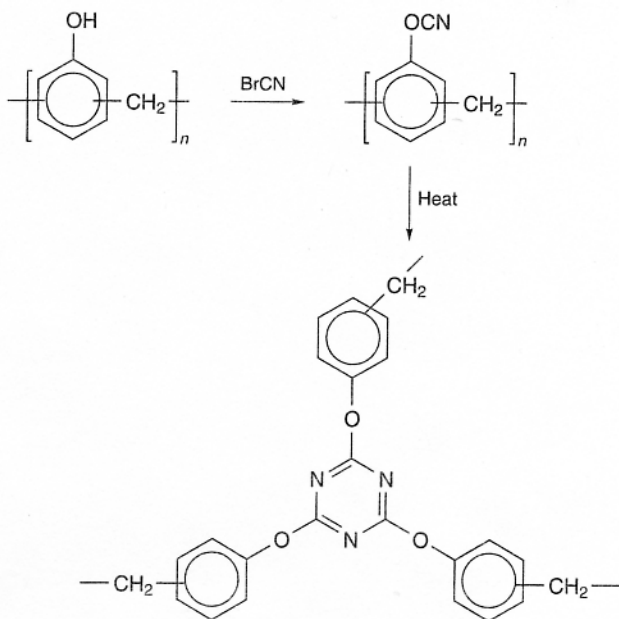


Figure 7.41 Synthesis of phenolic triazine resins.

amount of oxidation may occur in air as some carbonyl peaks have been observed using  $^{13}\text{C}$  NMR.<sup>108</sup>

Degradation in inert atmospheres between 300 and 600°C results in porous materials. Little shrinkage has been observed in this temperature range. Water, carbon monoxide, carbon dioxide, formaldehyde, methane, phenol, cresols, and xylenols are released. According to various thermogravimetric analyses, the weight loss rate reaches a maximum during this temperature range. The elimination of water at this stage may also be caused by the phenolic hydroxyl condensations which give rise to biphenyl ether linkages (Fig. 7.42).

Morterra and Low<sup>109,110</sup> proposed that thermal crosslinking may occur between 300°C and 500°C where phenolic hydroxyl groups react with methylene linkages to eliminate water (Fig. 7.43). Evidence for this mechanism is provided by IR spectra which show decreased OH stretches and bending absorptions as well as increased complexity of the aliphatic CH stretch patterns in this temperature range.

At elevated temperatures, methylene carbons cleave from aromatic rings to form radicals (Fig. 7.44). Further fragmentation decomposes xylenol to cresols and methane (Fig. 7.44a). Alternatively, auto-oxidation occurs (Fig. 7.44b). Aldehydes and ketones are intermediates before decarboxylation or decarbonylation takes place to generate cresols and carbon dioxide. These oxidative reactions are possible even in inert atmospheres due to the presence of hydroxyl radicals and water.<sup>5</sup>

Oxidative degradation begins at lower temperatures in air (<300°C) and oxidation occurs most readily on benzylic methylene carbons since they are the most

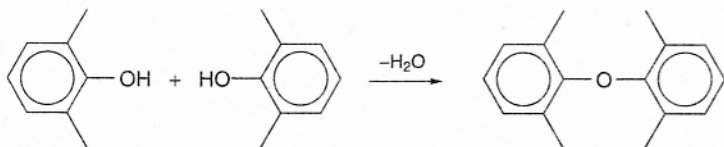


Figure 7.42 Dehydration of hydroxyl groups.

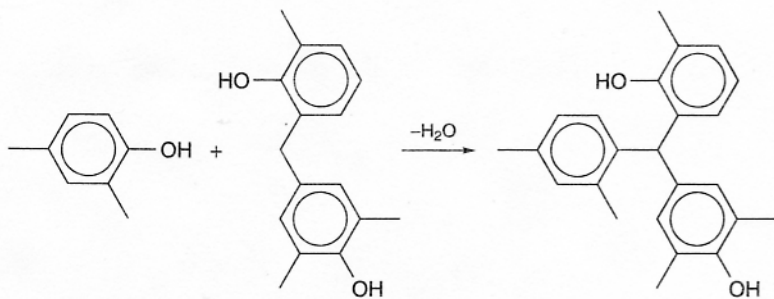
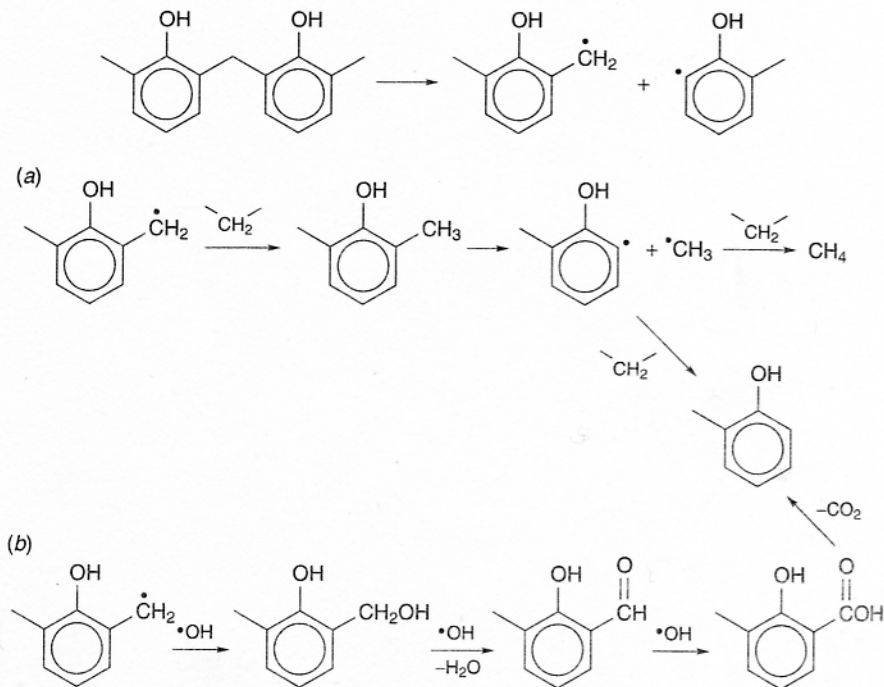


Figure 7.43 Thermal crosslinking of phenolic hydroxyl and methylene linkages.



**Figure 7.44** Thermal bond rupture: (a) fragmentation reaction. (b) oxidation degradation.

vulnerable sites. This leads to dihydroxybenzohydrole and dihydroxybenzophenone derivatives (Fig. 7.45). Dihydroxybenzophenone may cleave and further oxidize to carboxylic acid before decomposing to form cresols, xylenols,  $\text{CO}$ , and  $\text{CO}_2$ .

Hydroxyl elimination is necessary for the formation of benzaldehyde and benzoic acid derivatives and, ultimately, benzene and toluene (Fig. 7.46).<sup>2</sup> It is proposed that a cleavage between the hydroxyl group and aromatic ring leads to benzenoid species which undergo further cleavage coupled with oxidation to give various decomposition products.

Oxidative branching and crosslinking are the prevalent degradation pathways in air (Fig. 7.47). Phenoxy radicals are formed via hydrogen abstraction. These relatively stable intermediates can couple with each other and, depending on carbon-carbon or carbon-oxygen coupling, form ether linkages or ketones. Diphenolquinones derived from carbon-carbon dimerization further oxidize.<sup>2</sup>

Upon further heating above  $600^\circ\text{C}$ , the density increases as shrinkage occurs at a high rate. High-temperature degradation monitored via gas chromatography indicated that the formation of carbon char parallels carbon monoxide evolution. Along with the same by-products released at lower temperatures, pyrolysis gas chromatography/mass spectrometry (GC/MS) identified the formation of other

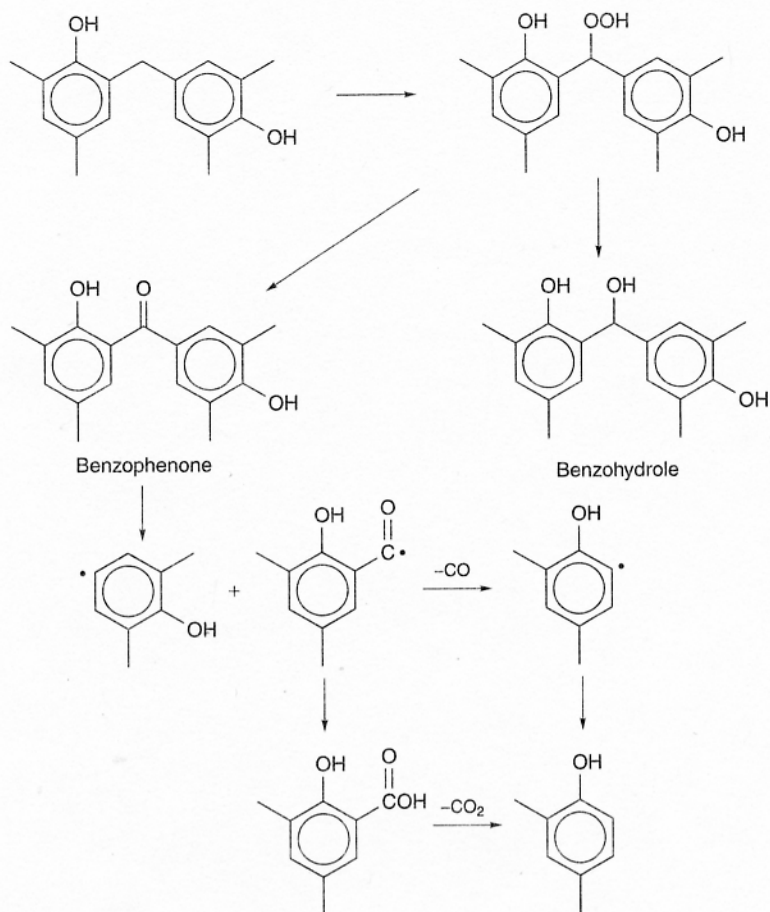


Figure 7.45 Oxidation degradation on methylene carbon.

low-volatility compounds, including naphthalene, methylnaphthalenes, biphenyl, dibenzofuran, fluorene, phenanthrene, and anthracene. These products may result from condensation of hydroxyl groups of adjacent ortho-ortho-linked phenolic rings<sup>111</sup> (Fig. 7.48).

The reaction sequence for char formation was also proposed to occur through the initial formation of quinone-type linkages, which lead to polycyclic products<sup>5</sup> (Fig. 7.49). The quinone functionalities were confirmed through IR studies. NMR spectra showed that at 400°C almost all methylene linkages and carbonyl groups shift or disappear. Mostly aromatic species are present. This is consistent with the proposed char-forming mechanism but is also compatible with the formation of biphenyls through direct elimination of CO.<sup>108</sup>

Conley showed that the primary degradation route for resole networks is oxidation regardless of the atmosphere.<sup>6</sup> By contrast, Morterra and Low found that

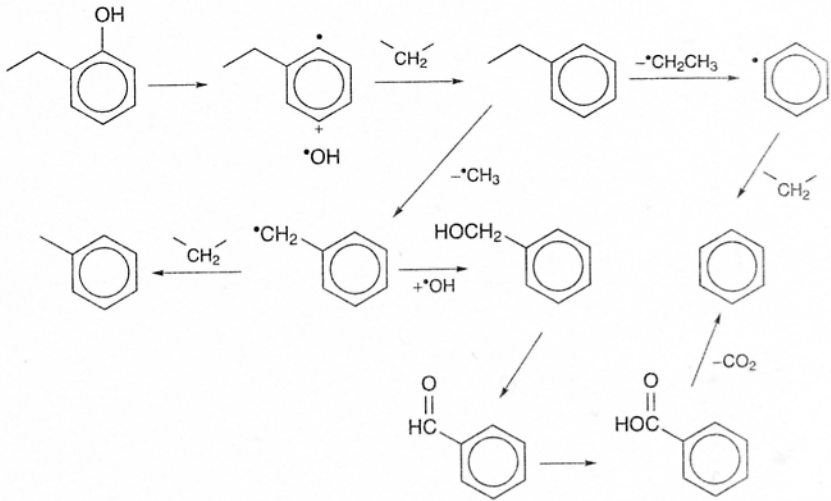


Figure 7.46 Formation of benzenoid species.

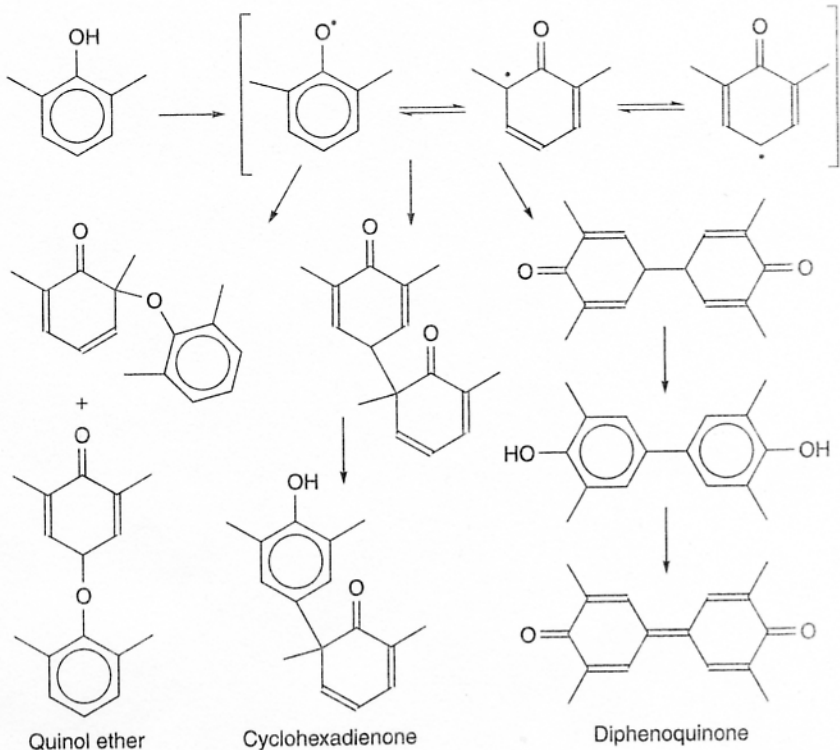


Figure 7.47 Decomposition via phenoxy radical pathways.

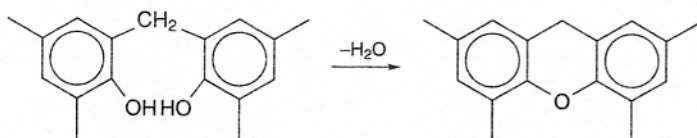


Figure 7.48 Condensation of ortho-hydroxyl groups.

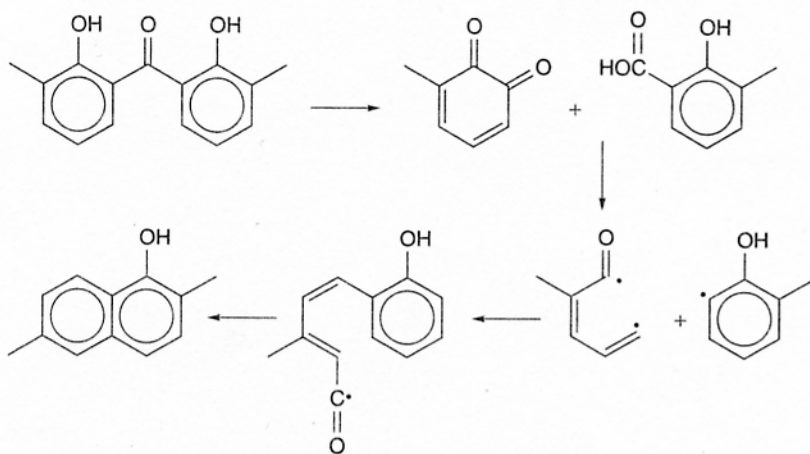


Figure 7.49 Char formation.

auto-oxidation was not the major degradation pathway for novolac resins.<sup>109</sup> The degradation is proposed to occur in two stages depending on the temperature. Fragmentation of the polymer chain, beginning at approximately 350°C, does not affect the polymer integrity. Above 500°C the network collapses as polyaromatic domains form.

Novolac network degradation mechanisms vary from those of resole networks due to differences in crosslinking methods. Nitrogen-containing linkages must also be considered when HMTA (or other crosslinking agent) was used to cure novolac networks. For example, tribenzylamines, formed in HMTA-cured novolac networks, decompose to cresols and azomethines (Fig. 7.50).

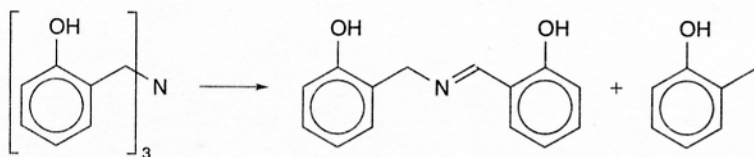


Figure 7.50 Decomposition of tribenzylamine.

Jha et al.<sup>112</sup> studied novolacs and networks which had been slowly heated in an inert atmosphere. Between 100 and 350°C, 1–2 wt % of water and phenol evolved. Above that temperature, small quantities of CO, CO<sub>2</sub>, CH<sub>4</sub>, and low-molecular-weight aromatics evolved, leaving behind 75–85% by weight of polymer. The degradation of these preexposed networks were then studied at temperatures up to ~700°C in both air and nitrogen. The rate of weight loss in air suggested that degradation under these conditions is a multistage process. Evidence suggested that this multistage thermo-oxidative process was due to two types of linking units present, which pyrolyzed at 375–400 and 500–550°C, respectively. By contrast, the degradation process in nitrogen was a single-stage process. Both processes formed a char representing 90–95% by weight of the preexposed materials. As expected, lower weight loss occurred with increased levels of the HMTA crosslinking reagent introduced into the network.

Oxygen indices of a series of phenolic networks (i.e., heat-cured resoles and novolacs cured with formaldehyde, trioxane, or terephthaloyl chloride) were investigated.<sup>113</sup> It has been previously shown that oxygen indices (OIs) correlate linearly with char yields at 800°C in nitrogen except for cases involving gas-phase retardants such as halogenated aromatic materials. The meta- and para-cresol formaldehyde networks exhibited slightly lower OI values than unsubstituted phenolics, presumably due to the presence of flammable methyl substituents. The halogenated phenolics showed higher OI values but lower char yields since halogenated materials undergo a gas-phase retardation of burning and the heavy halogen substituents convert to gaseous products. The crosslinking agent also has an effect on OI. Networks with methylene linkages derived from formaldehyde crosslinking reagents gave rise to higher OI values than those with ester linkages derived from terephthaloyl chloride. The formaldehyde-cured novolacs also showed higher OI than trioxane-cured materials since less stable ether linkages were formed in the trioxane crosslinked systems.

The effects of novolac structures and levels of crosslink densities on thermal stabilities were also investigated.<sup>114</sup> Three types of novolacs were prepared by reacting phenol with formaldehyde, meta-cresol with formaldehyde, and para-cresol with formaldehyde in a formaldehyde–phenol molar ratio of 0.95. Lightly crosslinked networks were obtained when the trifunctional phenol or meta-cresol was used. As expected, para-cresol novolac was linear. The thermal degradation behavior for the lightly crosslinked networks, the para-cresol novolac, as well as typical novolac resins were examined. Under inert atmosphere, thermogravimetric results revealed that the crosslinked samples had lower decomposition temperatures but the char yields were significantly higher. The greater stabilities exhibited at higher temperatures (500°C+) for the crosslinked materials were attributed to lesser fragmentation and, therefore, lower volatiles. In air, the crosslinked materials were less stable throughout the whole temperature range with complete degradation occurring 50°C below the low-molecular-weight resins. It was suggested that the crosslinked materials may be less susceptible to oxidation and, therefore, unable to form more thermally stable intermediates. Comparatively, the phenol–formaldehyde resin showed the highest thermal

and thermal oxidative stability, followed by the meta-cresol-formaldehyde resin. The para-cresol-formaldehyde showed the least stability. Since the reactivity of starting phenolic monomer was different, novolac oligomers prepared via the same approach resulted in different structures. The results obtained in this study therefore could not be compared quantitatively.

A low-molecular-weight para-cresol novolac resin ( $M_n \sim 560$ ) showed a high crystalline ratio according to X-ray diffraction.<sup>115</sup> No weight loss was observed below 400°C. However, the morphology changed to a semicrystalline state after repeat heating-cooling cycles.

## REFERENCES

1. *Society of Plastic Industries Facts and Figures*, SPI, Washington, DC, 1994.
2. A. Knop and L. A. Pilato, *Phenolic Resins—Chemistry, Applications and Performance*, Springer-Verlag, Berlin, 1985.
3. A. Knop and W. Scheib, *Chemistry and Application of Phenolic Resins*, Springer-Verlag, New York, 1979.
4. S. R. Sandler and W. Karo, *Polymer Synthesis*, 2nd ed., Vol. 2, Academic Boston, 1992.
5. P. W. Kopf, in *Encyclopedia of Chemical Technology*, 4th ed., Vol. 18, J. I. Kroschultz (Ed.), Wiley, New York, 1996, pp. 603–644.
6. R. T. Conley, *Thermal Stability of Polymers*, Marcel Dekker, New York, 1970, pp. 459–496.
7. K. Hultsch, *Am. Chem. Soc. Div. Organic Coating Plastic Chem.*, **26**(1), 121–128 (1966).
8. A. J. Norton, U.S. Patent 2,385,370, 1947; P. H. Phodes, U.S. Patent 2,385,372, 1946.
9. H. Diehm and A. Hit, "Formaldehyde," in *Ullmanns Encyclopadie der Techn. Chem.*, 4th ed. Vol. 11, Verlag Chemie, Weinheim, 1976.
10. C. M. Chen and S. E. Chen, *Forest Prod. J.*, **38**(5), 49–52 (1988).
11. A. J. Rojas and R. J. J. Williams, *J. Appl. Polym. Sci.*, **23**, 2083–2088 (1979).
12. N. J. L. Megson, *Chem.-Ztg.*, **96**(1–2), 15–19 (1972).
13. H. L. Bender, A. G. Farnharn, and J. W. Guyer, U.S. Patents 2,464,207 and 2,475,587, 1949.
14. W. Aubertson, U.S. Patent 4,113,700 (to Monsanto Co.), September 12, 1978.
15. G. Casnati, A. Pochini, G. Sartori, and R. Ungaro, *Pure Appl. Chem.*, **55**(11), 1677–1688 (1983).
16. P. J. de Bruyn, A. S. L. Lim, M. G. Looney, and D. H. Solomon, *Tetrahedron Lett.*, **35**(26), 4627–4630 (1994).
17. S. Lin, M. Rutnakornpituk, C. S. Tyberg, J. S. Riffle, and U. Sorathia, *Bridging the Centuries with SAMPE's Materials and Process Technology*, **45**(2), 1730–1743 (2000).
18. M. M. Sprung, *J. Appl. Polym. Sci.*, **63**(2), 334–343 (1941).

19. S. Miloshev, P. Novakov, V. I. Dimitrov, and I. Gitsov, *Chemtronics*, **4**, 251-253 (1989).
20. L. E. Bogan, Jr., "Understanding the Novolac Synthesis Reaction," in *Frontiers of Polymers and Advanced Materials*, P. N. Prasad (Ed.), Plenum, New York, 1994, pp. 311-318.
21. C. N. Cascaval, D. Rosu, and F. Mustata, *Eur. Polym. J.*, **30**(3), 329-333 (1994).
22. S. Miloshev, P. Novakov, V. I. Dimitrov, and I. Gitsov, *Polymer*, **32**(16), 3067-3070 (1991).
23. T. Yoshikawa, K. Kimura, and S. Fujimura, *Jo. Appl. Polym. Sci.*, **15**, 2513-2520 (1971).
24. T. A. Yamagishi, M. Nomoto, S. Ito, S. Ishida, and Y. Nakamoto, *Polym. Bull.*, **32**, 501-507 (1994).
25. L. E. Bogan, Jr., *Macromolecules*, **24**, 4807-4812 (1991).
26. M. G. Kim, W. L. Nieh, T. Sellers, Jr., W. W. Wilson, and J. W. Mays, *Ind. Eng. Chem. Res.*, **31**(3), 973-979 (1992).
27. F. L. Tobiason, C. Chandler, and F. E. Schwarz, *Macromolecules*, **5**(3), 321-325 (1972).
28. H. Mandal and A. S. Hay, *Polymer*, **38**(26), 6267-6271 (1997).
29. T. R. Dargaville, F. N. Guerzoni, M. G. Looney, D. A. Shipp, D. H. Solomon, and X. Zhang, *J. Polym. Sci. Pt. A: Polym. Chem.*, **35**(8), 1399-1407 (1997).
30. R. A. Pethrick and B. Thomson, *Br. Polym. J.*, **18**(3), 171-180 (1986).
31. B. Ottenbours, P. Adriaensens, R. Carleer, D. Vanderzande, and J. Gelan, *Polymer*, **39**(22), 5293-5300 (1998).
32. F. Y. Wang, C. C. M. Ma, and H. D. Wu, *J. Appl. Polym. Sci.*, **74**, 2283-2289 (1999).
33. P. P. Chu, H. D. Wu, and C. T. Lee, *J. Polym. Sci. Pt. B: Polym. Phys.*, **36**(10), 1647-1655 (1998).
34. H. D. Wu, C. C. M. Ma, and P. P. Chu, *Polymer*, **38**(21), 5419-5429 (1997).
35. H. D. Wu, P. P. Chu, C. C. M. Ma, and F. C. Chang, *Macromolecules*, **32**(9), 3097-3105 (1999).
36. H. D. Wu, C. C. M. Ma, P. P. Chu, H. T. Tseng, and C. T. Lee, *Polymer*, **39**(13), 2856-2865 (1998).
37. C. C. M. Ma, H. D. Wu, and C. T. Lee, *J. Polym. Sci. Pt. B: Polym. Phys.*, **36**(10), 1721-1729 (1998).
38. Z. Katovic and M. Stefanic, *Ind. Eng. Chem. Product Res. Devel.*, **24**, 179-185 (1985).
39. C. Holland, W. Stark, and G. Hinrichsen, *Acta Polym.*, **46**, 64-67 (1995).
40. P. W. Kopf and E. R. Wagner, *J. Polym. Sci. Polym. Chem. Ed.*, **11**(5), 939-960 (1973).
41. S. A. Sojka, R. A. Wolfe, and G. D. Guenther, *Macromolecules*, **14**, 1539-1543 (1981).
42. Y. Ogata and A. Kawasaki, "Equilibrium Additions to Carbonyl Compounds," in *The Chemistry of the Carbonyl Group*, J. Zabicky (Ed.), Vol. 2, Interscience, London, 1970.

43. T. R. Dargaville, P. J. De Bruyn, A. S. C. Lim, M. G. Looney, A. C. Potter, and D. H. Solomon, *J. Polym. Sci. Pt. A*, **35**, 1389–1398 (1997).
44. X. Zhang, M. G. Looney, D. H. Solomon, and A. K. Whittaker, *Polymer*, **38**(23), 5835–5948 (1997).
45. X. Zhang, A. C. Potter, and D. H. Solomon, *Polymer*, **39**(2), 399–404 (1998).
46. X. Zhang and D. H. Solomon, *Polymer*, **39**(2), 405–412 (1998).
47. X. Zhang, A. C. Potter, and D. H. Solomon, *Polymer*, **39**(10), 1957–1966 (1998).
48. X. Zhang, A. C. Potter, and D. H. Solomon, *Polymer*, **39**(10), 1967–1975 (1998).
49. X. Zhang and D. H. Solomon, *Polymer*, **39**(24), 6153–6162 (1998).
50. A. S. C. Lim, D. H. Solomon, and X. Zhang, *J. Polym. Sci. Pt. A: Polym. Chem.*, **37**, 1347–1355 (1999).
51. K. Lenghaus, G. G. Qiao, and D. H. Solomon, *Polymer*, **41**, 1973–1979 (2000).
52. J. H. Freemann and C. W. Lewis, *J. Am. Chem. Soc.*, **76**(8), 2080–2087 (1954).
53. A. A. Zsavitsas and R. D. Beaulieu, *J. Polym. Sci. A1*, **6**, 2451 (1969).
54. K. C. Eapen and L. M. Yeddanapalli, *Makromolek. Chem.*, **119**, 4 (1968).
55. M. F. Grenier-Loustalot, S. Larroque, P. Grenier, J. Leca, and K. Bedel, *Polymer*, **35**(14), 3046–3054 (1994).
56. M. F. Grenier-Loustalot, S. Larroque, P. Grenier, and D. Bedel, *Polymer*, **37**(6), 939–953 (1996).
57. B. Mechin, D. Hanton, J. Le Goff, and J. P. Tanneur, *Eur. Polym. J.*, **22**(2), 115–124 (1986).
58. M. F. Grenier-Loustalot, S. Larroque, P. Grenier, and D. Bedel, *Polymer*, **37**(6), 955–964 (1996).
59. L. Prokai, *J. Chromatogr.*, **333**(1), 91–98 (1985).
60. R. A. Haupt, and T. Sellers, *Ind. Eng. Chem. Res.*, **33**(3), 693–697 (1994).
61. M. F. Grenier-Loustalot, S. Larroque, D. Grande, P. Grenier, and D. Bedel, *Polymer*, **37**(8), 1363–1369 (1996).
62. G. Astarloa-Aierbe, J. M. Echeverria, A. Vazquez, and I. Mondragon, *Polymer*, **41**, 3311–3315 (2000).
63. B. D. Park and B. Riedl, *J. Appl. Polym. Sci.*, **77**(6), 1284–1293 (2000).
64. M. Grenier-Loustalot, S. Larroque, and P. Grenier, *Polymer*, **37**(4), 639–650 (1996).
65. T. Holopainen, L. Alvila, J. Rainio, and T. T. Pakkanen, *J. Appl. Polym. Sci.*, **69**(11), 2175–2185 (1998).
66. G. Carotenuto and L. Nicolais, *J. Appl. Polym. Sci.*, **74**(11), 2703–2715 (1999).
67. T. Holopainen, L. Alvila, J. Rainio, and T. T. Pakkanen, *J. Appl. Polym. Sci.*, **66**(6), 1183–1193 (1997).
68. M. G. Kim, L. W. Amos, and E. E. Barnes, *Ind. Eng. Chem. Res.*, **29**(10), 2032–2037 (1990).
69. P. Luukko, L. Alvila, T. Holopainen, J. Rainio, and T. T. Pakkanen, *J. Appl. Polym. Sci.*, **69**, 1805–1812 (1998).
70. T. Sellers and M. L. Prewitt, *J. Chromatogr.*, **513**, 271–278 (1990).
71. G. Gobec, M. Dunky, T. Zich, and K. Lederer, *Ang. Makromolek. Chem.*, **251**, 171–179 (1997).

72. M. G. Kim, W. L. Nieh, T. Sellers, W. W. Wilson, and J. W. Mays, *Ind. Eng. Chem. Res.*, **31**(3), 973–979 (1992).
73. G. Astarloa-Aierbe, J. M. Echeverria, J. L. Egiburu, M. Ormaetxea, and I. Mondragon, *Polymer*, **39**(14), 3147–3153 (1998).
74. L. Prokai and W. J. Simonsick, *Macromolecules*, **25**(24), 6532–6539 (1992).
75. J. M. Kenny, G. Pisaniello, F. Farina, and S. Puzziello, *Thermochim. Acta*, **269**, 201–211 (1995).
76. W. W. Focke, M. S. Smit, A. T. Tolmay, L. S. Vandervalt, and W. L. Vanwyk, *Polym. Eng. Sci.*, **31**(23), 1665–1669 (1991).
77. M. G. Kim, W. L. S. Nich, and R. M. Meacham, *Ind. Eng. Chem. Res.*, **30**(4), 798–803 (1991).
78. R. A. Follensbee, J. A. Koutsky, A. W. Christiansen, G. E. Myers, and R. L. Geimer, *J. Appl. Polym. Sci.*, **47**(8), 1481–1496 (1993).
79. M. J. Carrott and G. Davidson, *Analyst*, **124**(7), 993–997 (1999).
80. Y. Yazaki, P. J. Collins, M. J. Reilly, S. D. Terrill, and T. Nikpour, *Holzforschung*, **48**(1), 41–48 (1994).
81. J. Wolfrum and G. W. Ehrenstein, *J. Appl. Polym. Sci.*, **74**, 3173–3185 (1999).
82. L. B. Manfredi, O. de la Osa, N. Galego Fernandez, and A. Vazquez, *Polymer*, **40**, 3867–3875 (1999).
83. B. Tomita and C. Hse, *Mokuzai Gakkaishi*, **39**(11), 1276–1284 (1993).
84. B. Tomita, M. Ohyama, A. Itoh, K. Doi, and C. Hse, *Mokuzai Gakkaishi*, **40**(2), 170–175 (1994).
85. R. W. Biernath and D. S. Soane, "Cure Kinetics of Epoxy Cresol Novolac Encapsulant for Microelectronic Packaging," in *Contemporary Topic in Polymer Science. Advances in New Material*. Vol. 7, J. S. Salamone and J. S. Riffle (Eds.), Plenum, New York, 1992, pp. 103–160.
86. W. A. Romanchick, J. E. Sohn, and J. F. Geibel "Synthesis, Morphology, and Thermal Stability of Elastomer-Modified Epoxy Resin," in *ACS Symposium Series 221—Epoxy Resin Chemistry II*, R. S. Bauer (ed.), American Chemical Society, Washington DC, 1982, pp. 85–118.
87. D. Gagnebien, P. J. Madec, and E. Marechal, *Eur. Polym. J.*, **21**(3), 273–283 (1985).
88. W. G. Kim, J. Y. Lee, and K. Y. Park, *J. Polym. Sci. Pt. A: Polym. Chem.*, **31**, 633–639 (1993).
89. M. F. Sorokin and L. G. Shode, *Zhurnal Organicheskoi Khimii*, **2**(8), 1463–1468 (1966).
90. S. Han, H. G. Yoon, K. S. Suh, W. G. Kim, and T. J. Moon, *J. Polym. Sci. Pt. A: Polym. Chem.*, **37**, 713–720 (1999).
91. C. S. Chern and G. W. Poehlein, *Polym. Eng. Sci.*, **27**(11), 788–795 (1987).
92. X. W. Luo, Z. H. Ping, J. P. Ding, Y. D. Ding, and S. J. Li, *Pure Appl. Chem.*, **A34**(11), 2279–2291 (1997).
93. C. S. Tyberg, M. Sankarapandian, K. Bears, P. Shih, A. C. Loos, D. Dillard, J. E. McGrath, and J. S. Riffle, *Construct. Build. Mater.*, **13**, 343–353 (1999).
94. C. S. Tyberg, K. Bergeron, M. Sankarapandian, P. Shih, A. C. Loos, D. A. Dillard, J. E. McGrath, and J. S. Riffle, *Polymer*, **41**(13), 5053–5062 (2000).

95. C. S. Tyberg, P. Shih, K. N. E. Verghese, A. C. Loos, J. J. Lesko, and J. S. Riffle, *Polymer*, **41**, 9033–9048 (2000).
96. M. Ochi, N. Tsuyuno, K. Sakaga, Y. Nakanishi, and Y. Murata, *J. Appl. Polym. Sci.*, **56**, 1161–1167 (1995).
97. T. Suzuki, Y. Oki, M. Numajiri, T. Miura, K. Kondo, Y. Shiomi, and Y. Ito, *J. Appl. Polym. Sci.*, **49**, 1921–1929 (1993).
98. W. J. Burke, E. L. M. Glennie, and C. Weatherbee, *J. Organic Chem.*, **29**, 909 (1964).
99. X. Ning and H. Ishida, *J. Polym. Sci. Pt. A: Polym. Chem.*, **32**, 1121–1129 (1994).
100. H. Ishida and Y. Rodriguez, *Polymer*, **36**(16), 3151–3158 (1995).
101. G. Riess, J. M. Schwob, G. Guth, M. Roche, and B. Lande, "Ring Opening Polymerization of Benzoxazines—A New Route to Phenolic Resins," in *Advances in Polymer Synthesis*, B. M. Culbertson and J. E. McGrath (Eds.), Plenum, New York, 1985, pp 27–50.
102. J. Dunkers and H. Ishida, *J. Polym. Sci. Pt. A: Polym. Chem.*, **37**(13), 1913–1921 (1999).
103. H. Ishida and D. J. Allen, *J. Polym. Sci. Polym. Phys. Ed.*, **34**(6), 1019–1031 (1996).
104. Y. X. Wang and H. Ishida, *Polymer*, **40**(16), 4563–4570 (1999).
105. S. Das and D. C. Prevorsek, U.S. Patent 4,831,086 (to Allied-Signal, Inc.), May 16, 1989.
106. S. Das, *Abstr. Pap. Am. Chem. Soc.—PMSE*, **203**, 259 (1992).
107. C. P. R. Nair, R. L. Bindu, and V. C. Joseph, *J. Polym. Sci. Pt. A: Polym. Chem.*, **33** (4), 621–627 (1995).
108. C. A. Fyfe, M. S. McKinnon, A. Rudin, and W. J. Tchir, *Macromolecules*, **16**, 1216–1219 (1983).
109. C. Morterra and M. I. D. Low, *Carbon*, **23**(5), 525–530 (1985).
110. C. Morterra and M. I. D. Low, *Langmuir*, **1**, 320–326 (1985).
111. J. Hetper and M. Sobera, *J. Chromatogr. A*, **833**, 277–281 (1999).
112. V. Jha, A. Banthia, and A. Paul, *J. Thermal Anal.*, **35**, 1229–1235 (1989).
113. Y. Zaks, J. Lo, D. Raucher, and E.M. Pearce, *J. Appl. Polym. Sci.*, **27**, 913–930 (1982).
114. L. Costa, L. Rossi di Montelera, G. Camino, E. D. Weil, and E. M. Pearce, *Polym. Degrad. Stabil.*, **56**, 27–35 (1997).
115. A. Hamou, C. Devallencourt, F. Burel, J. M. Saiter, and M. Belbachir, *J. Thermal Anal.*, **52**, 697–703 (1998).

## 7.9 APPENDIX

The procedures which follow were adapted from *Polymer Synthesis*, 2nd ed., Vol. II, by S. R. Sandler and W. Karo, Academic, New York, 1992.

### 7.9.1 Preparations of Phenol-Formaldehyde Resole Resins

#### 7.9.1.1 Method A

Eight hundred grams (8.5 mol) of phenol, 80.0 g water, 940.5 g 37 wt % aqueous formaldehyde (11.6 mol), and 40 g of barium hydroxide octahydrate were charged to a resin kettle. The reaction mixture was maintained at 70°C for 2 h with stirring; then sufficient oxalic acid was added to bring the pH to 6–7. The resinous material was partially condensed by removing water at 30–50 mm Hg at a temperature no higher than 70°C. Samples (1–2 mL) were withdrawn every 15 min to check the extent of condensation. The endpoint was taken when a sample of resin placed on a hot plate at 160°C gelled in less than 10 s or when the cooled resin was brittle and “nontacky” at room temperature. The resin at this point was termed an A-stage resole. Further heating converts this into a B-stage and finally to a C-stage resin.

#### 7.9.1.2 Method B

Forty-seven grams (0.5 mol) of phenol, 80 mL of 37 wt % aqueous formaldehyde (1.0 mol), and 100 mol of 4 N NaOH were charged to a flask equipped with a reflux condenser and mechanical stirrer. The reaction mixture was stirred at room temperature for 16 h, then heated on a steam bath for 1 h. The mixture was cooled and the pH adjusted to 7.0. The aqueous layer was decanted from the viscous brown liquid product, the wet organic phase was taken up in 500 mL of acetone and dried over anhydrous MgSO<sub>4</sub>, then over molecular sieves. The dried acetone product solution was filtered and evaporated to yield a water-free light brown syrup.

### 7.9.2 Preparation of Phenol-Formaldehyde Novolac Resin

Twenty-four hundred grams (25.6 mol) of phenol, 1645 g of 37 wt % formaldehyde (20.3 mol), and 30 g (0.33 mol) of oxalic acid were charged to a 5-L, three-necked resin kettle. The mixture was stirred and refluxed until the distillate was free of formaldehyde (1–3 h); then water was distilled from the mixture until the resin temperature reached 154°C. The viscosity of the resin at this point at 150°C was such that 105 s was required for flow in an inclined plate test. The pressure was slowly reduced while a slow current of nitrogen was bubbled through the resin, and the mixture was heated to 175°C at 6 mm Hg. Approximately 6 wt % phenol was recovered; then the resin was poured into an aluminum dish and cooled. The resin had a melt viscosity of 510 s at 150°C.